

Author's Response

Delivery of halogenated very short-lived substances from the West Indian Ocean to the stratosphere during Asian summer monsoon

Alina Fiehn^{1,2}, Birgit Quack², Helmke Hepach^{2,*}, Steffen Fuhlbrügge², Susann Tegtmeier², Matthew Toohey², Elliot Atlas³, Kirstin Krüger¹

¹*Meteorology and Oceanography Section, Department of Geosciences, University of Oslo, Oslo, Norway*

²*GEOMAR Helmholtz Centre for Ocean Research Kiel, Kiel, Germany*

³*Rosenstiel School of Marine and Atmospheric Science, University of Miami, Miami, USA*

* *now at: Environment Department, University of York, York, United Kingdom*

Answers to Reviewer Comment 1

We would like to thank Reviewer 1 for the comments to improve the manuscript. Below, you find our answers to the specific points. The reviewer's comment is written in *italic letters*, our answer in normal font.

Summarizing, the paper is well-written and presents an important contribution to our understanding of transport of the short-lived species from the boundary layer over the West Indian Ocean into the stratosphere. It should be published after some minor revisions.

We thank the reviewer for this very positive review.

Answers to the specific comments of the reviewer:

This leads to my first critical remark: The authors claim, that the value of 17 km height for the location of the tropopause represents the average cold point tropopause during the cruise and for the whole tropical region. [...] But why not using a tropopause location computed from the ERA Interim data, the same data underlying the transport calculation? I am not doubting the general location of the maximum entrainment areas, but using the ERA Interim based tropopause would be much more convincing and more consistent.

We tested several definitions for stratospheric entrainment for our trajectory runs. Flexpart includes the lapse rate tropopause (LRT) calculation after the WMO (1957) definition. Using our Flexpart/ERA-Interim trajectory runs this tropopause lies lower (14-15 km, see Fig. R1 below) than the one we observed during the cruise (17.0 km Fig S2 from paper) and the one inferred from satellite measurements during JJA at the equator (LRT 16.2 km, cold point tropopause (CPT) 16.7 km (Munchak and Pan, 2014)). In the Asian monsoon anticyclone the tropopause lies even higher between 17.2 (LRT) and 17.6 km (CPT) height for a 4 year mean (Munchak and Pan, 2014). A temperature threshold of 192 K (average CPT temperature over the Indian monsoon region in JJA (Kim and Son, 2012)) lead to a tropopause height around 16.5 km (Fig. R1). Thus, we decided to use 17 km height as a conservative approximation to the tropical tropopause height over the Indian Ocean and Asia during boreal summer and added other entrainment altitudes (13, 15, 18 km) in the supplementary material.

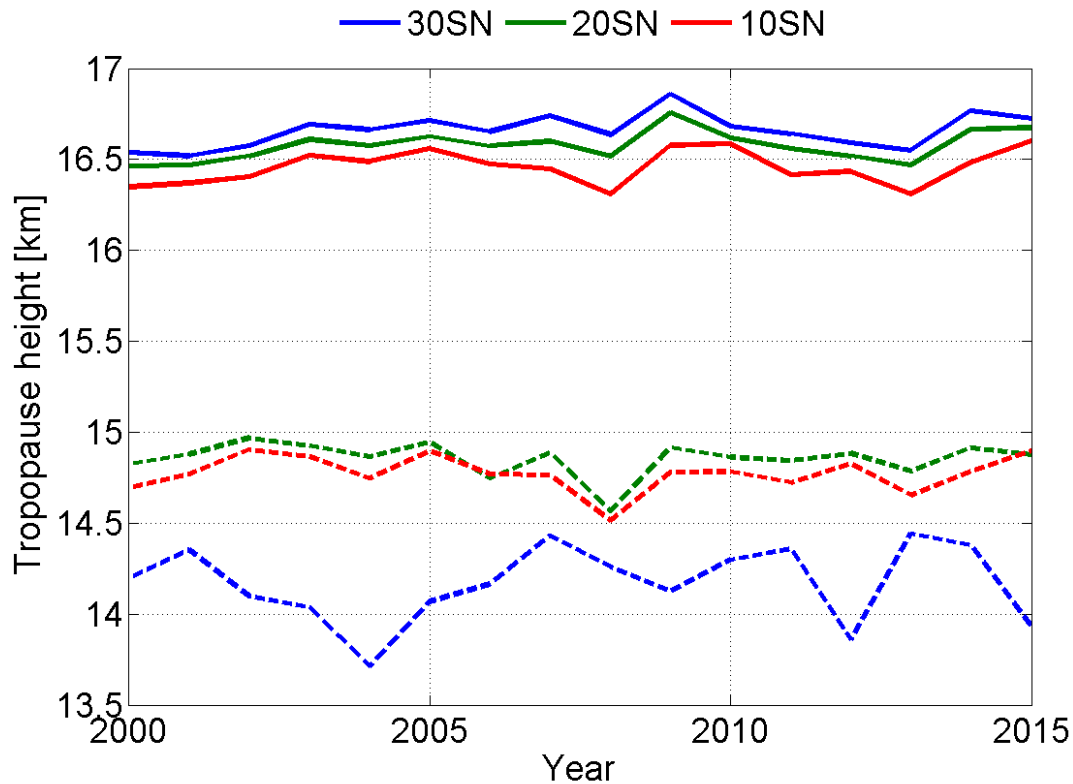


Figure R1: Height of trajectories at entrainment locations using different tropopause definitions. Dashed lines show the lapse rate tropopause from ERA-Interim, and solid lines the height of trajectories reaching temperatures below 192 K. 30SN means stratospheric entrainment between 30°S and 30°N and so on.

Speaking of this, ERA Interim provides much higher horizontal resolution than used. Why not using it for better, more accurate trajectory results, better resolved convection and better tropopause location? Even the Flexpart parameterizations for vertical transport and convection could benefit from this.

The spatial resolution of the current available **ECMWF reanalysis from 1979 onwards**, ERA-Interim, is approximately 80 km in grid space (T255 triangular truncation) on 60 vertical levels from the surface up to 0.1 hPa. Thus the chosen 1°x1° grid resolution (111 km at the equator) is very close to the original model resolution. Higher spatial and vertical resolution ECMWF data is only available from the operational model with T1279 and L137 (since 2010 and 2013 respectively). However, the high resolution operational model was not suitable for our study on a longer interannual time series due to regular changes of the operational ECWMMF weather model in order to improve the forecast.

To investigate more on stratospheric entrainment and the role of the West Indian Ocean a third forward trajectory model run is started with domain filling trajectories from a rectangular area over the area of interest (Indian Ocean setup). In this context now VLS tracers are used, which undergo an exponential decay according to certain tropical tropospheric life times. This is in contrast to the vertical life time profile used for the simple OASIS setups, and I am not sure, why there are two different life times used. May be the authors can comment on this.

The two calculation methods differ slightly from each other in their timing of the calculation of compound decay. For the first method, the VLS **emissions** are attached to the trajectories and the decay is calculated online with the model. The height of the particle position is known and can be used for determination of lifetime according to the vertical profile. For the second approach, the VLS **tracer** transport is attributed to a trajectory after the model has been run by considering the transport time. We added the following explanatory sentence in line 264: “The use of VLS tracers allows us to evaluate one model run for different compounds with varying lifetimes.”

There is one more remark about the investigations with respect to the spatial variability of the stratospheric entrainment: In line 502 the definition of two core entrainment areas are mentioned, which are assumed to be evenly sized (and are shown in Fig. 6). It should be noted that these two regions may be evenly sized in grid space (that is 20 x 25 degrees), but not in area. Furthermore just by looking at the plots, one could think of moving the core entrainment box for the local convection 5 degrees more to the east for a better capture of entrainment. But maybe these boxes are chosen to be similar to Chen et al. (2012). If this is the case, it should be mentioned.

Thanks for this comments. Yes it is true. Geographically, the entrainment areas are not evenly sized. We reformulated to “... and to be evenly sized in grid space” in line 502. The entrainment areas were not chosen to be similar to Chen et al. (2012). We will furthermore move the Local Convection entrainment area 5° to the east. This will also lead to changes in Fig. 6, Table 6 and the numbers in Sect. 4.2.

In the last part of the study the simulation with the Indian Ocean setup is extended to 16 years to specify inter-annual variability. To quantify the influence of different transport regimes (local convection and Asian monsoon) on the total entrainment, the respective time series are correlated by using Pearsons correlation coefficient. It should be noted, that for all values not -1 or 1 Pearsons r is not meaningful, as long as there is no linearity between the two times series and/or if the values are not normally distributed. If there is a linear relationship, than correlation coefficients of 0.54 and 0.56 only explain 29% and 32% of the observed variance, meaning that roughly 70% of the variance is not explained. Even for a value of 0.87 (as for CH₃I) just 75% of the variance are explained. To decide, whether these values are significant, you need to do a t test. A much more robust method, which does not imply linearity, but only monotonicity is Spearman’s rank correlation coefficient. There is a similar method introduced by Kendall. I would

recommend to use one of these rank correlation coefficients, which is fairly easy to do, but would give more meaningful results.

Thanks for this discussion. We checked all our time series for normal distribution. They are normally distributed and thus Pearson correlations can be applied. Then we calculated p-values to infer the significance of the correlations in Table 6. We marked all 95% significant correlations in bold face. We also calculated the Spearman's rank correlation coefficients. These differed less than 0.1 from the Pearson correlation coefficients and thus we would like to continue using the Pearson correlation. The following sentence is added to Sect. 2.2: " We calculated the p-value to determine the 95% significance level of the correlations."

The values shown in figure 6 are labeled as tracer density (given in percent). Is this meant to be the same as tracer entrainment?

Yes, it is meant to be tracer entrainment, but the relative distribution of this tracer entrainment. So it could also be named relative tracer entrainment, or entrainment density. We changed the label in Fig. 6 to "entrainment density".

Citations

Kim, J., and Son, S.-W.: Tropical Cold-Point Tropopause: Climatology, Seasonal Cycle, and Intraseasonal Variability Derived from COSMIC GPS Radio Occultation Measurements, *Journal of Climate*, 25, 5343-5360, 10.1175/jcli-d-11-00554.1, 2012.

Munchak, L. A., and Pan, L. L.: Separation of the lapse rate and the cold point tropopauses in the tropics and the resulting impact on cloud top-tropopause relationships, *Journal of Geophysical Research: Atmospheres*, 119, 7963-7978, 10.1002/2013jd021189, 2014.

WMO: Definition of the tropopause, *WMO Bull.*, 6, 136, 1957.

Answers to Reviewer Comment 2

We would like to thank Reviewer 2 for the suggestions to further improve the manuscript. Below you find our answers to your specific points. The reviewer's comment is written in *italics*, our answer in normal font.

Overall I think this is a good paper and should be published in ACP. There is considerable interest in short-lived halocarbon emissions and the cruise presented here provides important additional information. The stratospheric input is quantified and presented with a range of model-based metrics which allow comparison with other studies. The uncertainties/limitations of the modeling are described.

We thank the reviewer for this very positive review.

Answers to the specific comments of the reviewer:

Line 130: The word 'project' is not correct here. (Also line 466).

In line 130, we changed 'project' to 'model'. In line 466, 'projected' was changed to 'determined'.

Line 136: '..during the Asian summer monsoon season'? (Missing words?)

The term summer monsoon already includes one season. We thus think that the word "season" is not necessary in the manuscript.

Line 193: Do you mean 154 samples every 3 hours, or 154 overall which are spaced about every 3 hours?

We mean 154 overall samples spaced about every 3 hours. We added "overall" and "spaced about" to the sentence.

"Line 257: 'July 2000-2015'. Should be rewritten to clarify it is for July during those years.

Done.

Line 283: Can you show these differences with respect to the ECMWF winds somehow?

Figure 1a shows the ECMWF monthly mean winds as black arrows and the in situ ship measurements as blue arrows. Thus, we think differences are directly visible in the figure. See also our answer to your next comment.

Can you add the time varying ECMWF winds in Figure 2, if there is a discrepancy to discuss?

The comparison of time varying ERA-Interim winds and in situ ship winds can be found in Fig. S1 in the supporting material. In line 285, we added the sentence: “Surface winds from in situ ship measurements, radiosondes, and time varying ERA-Interim data show good agreement (Fig. S1).”

Line 291: Give the lifetime of butane so the reader can judge what this is testing.

The atmospheric lifetime of butane is estimated to 2.5 days considering the reaction with OH and ozone (Finlayson-Pitts and Pitts, 2000). We added to line 291: “(lifetime 2.5 days; Finlayson-Pitts and Pitts, 2000)”.

Line 301: Change ‘lower’ to ‘smaller’. (There are many other places where I would suggest changing higher to larger, when higher can be confused with meaning higher altitude).

Yes, we agree with the reviewer and changed the words “lower” and “higher” in several places in Sect. 3.2 and 3.3 to “smaller” and “larger/stronger”, respectively.

Section 3.3.: This section compares the emission values between the cruises, but I think it is missing an overall synthesis or discussion about what these differences tell us about the different regimes or techniques. I would suggest adding a paragraph after line 389.

We added the following paragraph at line 389: “In general, the emissions measured during the OASIS cruise in the subtropical and tropical West Indian Ocean were as large as or larger than in other tropical open ocean cruises or studies. Especially CH₂Br₂ emissions during the OASIS cruise were larger than any previous emission estimates. The West Indian Ocean seems to be a region with significant contribution to the global open ocean VSLs emissions, especially in boreal summer when wind speeds are high because of the southwest monsoon circulation.”

Line 398: It would be interesting to see some plot of the vertical distribution of tracers in the different transport regimes.

We show the vertical distribution of bromoform from the OASIS cruise for the four transport regimes averaged over the time of the model calculation in the below Fig. R2. These profiles confirm that the bromoform emissions in the Westerlies and Transitions regime stay mostly below 5 km height, while in the Monsoon Circulation and Local Convection regimes bromoform is more uniformly distributed in the troposphere. We added this figure to the supporting material and explanatory text in line 404: “The different uplift heights are reflected in the vertical distribution of bromoform in each transport regime (Fig. S2).”

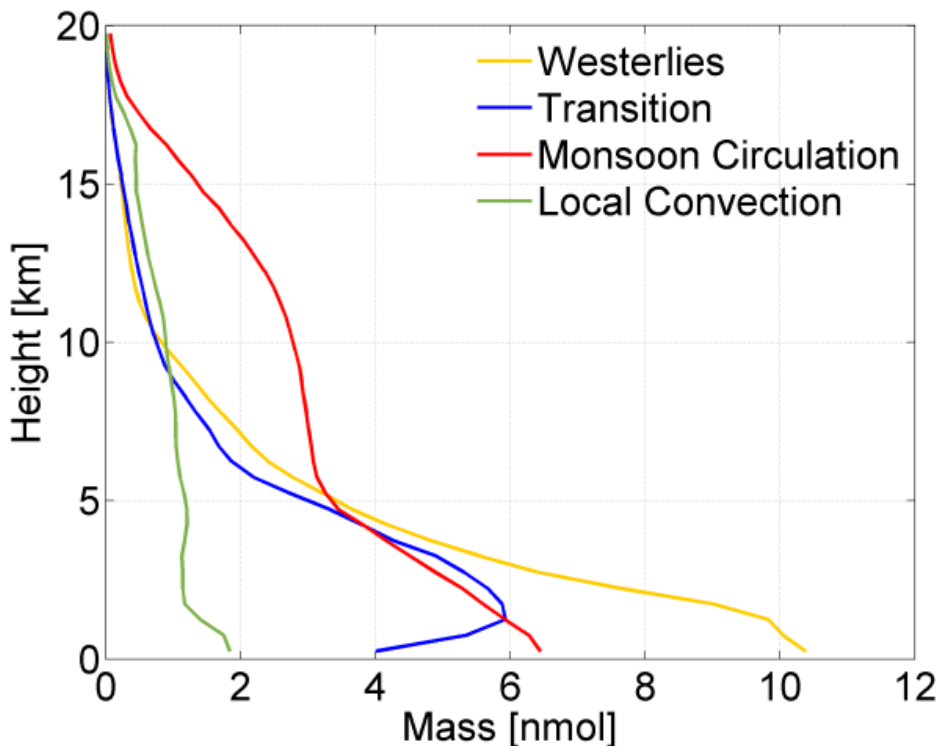


Figure R2: Time-averaged vertical distribution of bromoform in the four transport regimes (Figure 3b).

Line 413: I don't understand the definition of transit half-life. It might be the use of 'has reached 17km.' All entrained tracer reaches 17km? It seems like Figure 5 would help but that comes later. For Figure 5 can you add a symbol on the blue line at the half-life value? (If I have understood correctly).

We used the term “entrained tracer” as a synonym for “has reached 17 km”. We changed the explanation to: “...transit half-life, which is the time after which half of the total amount of entrained tracers have been entrained above 17 km altitude.” We also added a half-life marker in Fig. 5.

Line 416: Table 4: Please check all the values in Table 4. I tried to check my understanding of Transport Efficiency by dividing entrainment by emission. E.g. for CHBr₃ cruise mean: $5.5/430 =$

1.28%. Not 1.38. I tried other values and there seemed to be differences (23.6/430 = 5.49% and not 6.38%). What is wrong? Also, it would help if the text used the same precision as the table (e.g. line 419 say 1.38% and not 1.3%, or is it 1.28%?).

Thanks for checking Table 4 carefully! Your understanding of the transport efficiency is correct. There were slips in Table 4, because of a former version of the manuscript. We recalculated transport efficiencies, corrected the tables and adjusted the precision in the table and Sect. 3.4.

Figure 5: What are the units of the left-hand y axis?

The unit on this axis is number. We added the unit to the y-axis description of Fig. 5.

References

Finlayson-Pitts, B., and Pitts, J.: Chemistry of the upper and lower atmosphere: Theory, experiments and applications, Academic, US, 2000.

Changes made to the manuscript

- Table 4 was corrected.
- Fig. 5 was updated.
- We moved the Local Convection area in Fig. 6. This lead to changes in Fig.6, Table 6, and Sect. 4.2.
- Figure R2 was added to the supporting material.
- Minor changes were made according to the Answers to the Reviewers.

5

Delivery of halogenated very short-lived substances from the West Indian Ocean to the stratosphere during Asian summer monsoon

10 Alina Fiehn^{1,2}, Birgit Quack², Helmke Hepach^{2,*}, Steffen Fuhlbrügge², Susann Tegtmeier², Matthew Toohey², Elliot Atlas³, Kirstin Krüger¹

¹*Meteorology and Oceanography Section, Department of Geosciences, University of Oslo, Oslo, Norway*

²*GEOMAR Helmholtz Centre for Ocean Research Kiel, Kiel, Germany*

15 ³*Rosenstiel School of Marine and Atmospheric Science, University of Miami, Miami, USA*

^{*}*now at: Environment Department, University of York, York, United Kingdom*

Alina Fiehn: alina.fiehn@geo.uio.no
20 Birgit Quack: bquack@geomar.de
Helmke Hepach: hhepach@geomar.de
Steffen Fuhlbrügge: sfuhlbruegge@geomar.de
Susann Tegtmeier: stegtmeier@geomar.de
Matthew Toohey: mtoohey@geomar.de
25 Elliot Atlas: eatlas@rsmas.miami.edu
Kirstin Krüger: kkruieger@geo.uio.no (corresponding author)

Abstract

30 Halogenated very short-lived substances (VSLS) are naturally produced in the ocean and emitted to the atmosphere. When transported to the stratosphere, these compounds can have a significant influence on the ozone layer and climate. During a research cruise on RV *Sonne* in the subtropical and tropical West Indian Ocean in July and August 2014, we measured the VSLS, methyl iodide (CH_3I) and for the first time bromoform (CHBr_3) and dibromomethane (CH_2Br_2),
35 in surface seawater and the marine atmosphere to derive their emission strengths. Using the Lagrangian transport model Flexpart with ERA-Interim meteorological fields, we calculated the direct contribution of observed VSLS emissions to the stratospheric halogen burden during Asian summer monsoon. Furthermore, we compare the in situ calculations with the interannual variability of transport from a larger area of the West Indian Ocean surface to the stratosphere for
40 July 2000-2015. We found that the West Indian Ocean is a strong source region for CHBr_3 ($910 \text{ pmol m}^{-2} \text{ h}^{-1}$), very strong for CH_2Br_2 ($930 \text{ pmol m}^{-2} \text{ h}^{-1}$), and average for CH_3I ($460 \text{ pmol m}^{-2} \text{ h}^{-1}$). The atmospheric transport from the tropical West Indian Ocean surface to the stratosphere experiences two main pathways. On very short timescales, especially relevant for the shortest-lived compound CH_3I (3.5 days lifetime), convection above the Indian Ocean lifts
45 oceanic air masses and VSLS towards the tropopause. On a longer timescale, the Asian summer monsoon circulation transports oceanic VSLS towards India and Bay of Bengal, where they are lifted with the monsoon convection and reach stratospheric levels in the southeastern part of the Asian monsoon anticyclone. This transport pathway is more important for the longer-lived brominated compounds (17 and 150 days lifetime for CHBr_3 and CH_2Br_2). The entrainment of
50 CHBr_3 and CH_3I from the West Indian Ocean to the stratosphere during Asian summer monsoon is less than from previous cruises in the tropical West Pacific Ocean during boreal autumn/early winter, but higher than from the tropical Atlantic during boreal summer. In contrast, the projected CH_2Br_2 entrainment was very high because of the high emissions during the West Indian Ocean cruise. The 16-year July time series shows highest interannual variability for the short-lived CH_3I
55 and lowest for the long-lived CH_2Br_2 . During this time period, a small increase of VSLS entrainment from the West Indian Ocean through the Asian monsoon to the stratosphere is found. Overall, this study confirms that the subtropical and tropical West Indian Ocean is an important source region of halogenated VSLS, especially CH_2Br_2 , to the troposphere and stratosphere during the Asian summer monsoon.

60 1 Introduction

Natural halogenated volatile organic compounds in the ocean originate from chemical and biological sources like phytoplankton and macro algae (Carpenter et al., 1999;Quack and Wallace, 2003;Moore and Zafiriou, 1994;Hughes et al., 2011). When emitted to the atmosphere, the halogenated very short-lived substances (VSLS) have atmospheric lifetimes of less than half a
65 year (Law et al., 2006). Current estimates of tropical tropospheric lifetimes are 3.5, 17, and 150 days for methyl iodide (CH_3I), bromoform (CHBr_3), and dibromomethane (CH_2Br_2), respectively (Carpenter et al., 2014). VSLS can be transported to the stratosphere by tropical deep convection, where they contribute to the halogen burden, take part in ozone depletion and thus impact the climate (Solomon et al., 1994;Dvortsov et al., 1999;Hossaini et al., 2015).

70 CHBr_3 is an important biogenic VSLS due to its large oceanic emissions and because it carries three bromine atoms per molecule into the atmosphere (Quack and Wallace, 2003;Hossaini et al., 2012). CH_2Br_2 has a longer lifetime than CHBr_3 , and thus a higher potential for stratospheric entrainment. CH_3I is an important carrier of organic iodine from the ocean to the atmosphere and the most abundant organic iodine compound in the atmosphere (Manley et al.,
75 1992;Moore and Groszko, 1999;Yokouchi et al., 2008). Despite its very short atmospheric lifetime, it can deliver iodine to the stratosphere in tropical regions (Solomon et al., 1994;Tegtmeier et al., 2013). Ship-based observations showed that bromocarbon emissions near coasts and in oceanic upwelling regions are generally higher than in the open ocean, because of macro algal growth near coasts (Carpenter et al., 1999) and enhanced primary production in
80 upwelling regions (Quack et al., 2007), while coastal anthropogenic sources also need to be considered (Quack and Wallace, 2003;Fuhlbrügge et al., 2016b). Measurements of VSLS in the global oceans are sparse and the data shows a large variability. Thus, attempts at creating observation based global emission estimates and climatologies (bottom-up approach) (Quack and Wallace, 2003;Butler et al., 2007;Palmer and Reason, 2009;Ziska et al., 2013), modeling the
85 global distribution of halogenated VSLS emissions from atmospheric abundances (the top-down approach) (Warwick et al., 2006;Liang et al., 2010;Ordóñez et al., 2012), as well as biogeochemical modeling of oceanic concentrations (Hense and Quack, 2009;Stemmler et al., 2014) are subject to large uncertainties (Carpenter et al., 2014). Global modeled top-down estimates (Warwick et al., 2006;Liang et al., 2010;Ordóñez et al., 2012) yield higher emissions

90 than bottom-up estimates (Ziska et al., 2013;Stemmler et al., 2014, 2015), which may indicate the importance of localized emission hot spots underrepresented in current bottom-up estimates.

The amount of oceanic bromine from VSLS entrained into the stratosphere is estimated to be 2-8 ppt, which is 10-40 % of the currently observed stratospheric bromine loading (Dorf et al., 2006;Carpenter et al., 2014). This wide range results mainly from uncertainties in tropospheric
95 degradation and removal, transport processes, and especially from the spatial and temporal emission variability of halogenated VSLS (Carpenter et al., 2014;Hossaini et al., 2016). Analyzing the time period 1993-2012, Hossaini et al. (2016) found no clear long-term transport-driven trend in the stratospheric injection of oceanic bromine sources during a multi-model intercomparison.

100 Transport processes strongly impact stratospheric injections of VSLS, because their lifetimes are comparable to tropospheric transport timescales from the ocean to the stratosphere. The main entrance region of tropospheric air into the stratosphere is above the tropical West Pacific. Another active region lies above the Asian monsoon region during boreal summer (Newell and Gould-Stewart, 1981), when the Asian monsoon circulation provides an efficient
105 transport pathway from the atmospheric boundary layer to the lower stratosphere (Park et al., 2009;Randel et al., 2010). Above India and the Bay of Bengal, convection lifts boundary layer air rapidly into the upper troposphere (Park et al., 2009;Lawrence and Lelieveld, 2010). As a response to the persistent deep convection, an anticyclone forms in the upper troposphere and lower stratosphere above Central, South and East Asia (Hoskins and Rodwell, 1995). This so-called Asian monsoon anticyclone confines the air masses that have been lifted to this level
110 within the anticyclonic circulation (Park et al., 2007;Randel et al., 2010). For the period 1951-2015, a decreasing trend in rainfall and thus convection has been reported over northeastern India caused by a weakening northward moisture transport over the Bay of Bengal (Latif et al., 2016).

115 Chemical transport studies in the Asian monsoon region have mostly focused on water vapor entrainment to the stratosphere (Gettelman et al., 2004;James et al., 2008), or the transport of anthropogenic pollution (Park et al., 2009). The chemical composition and source regions for air masses in the Asian monsoon anticyclone have been the topic of more recent studies (Bergman et al., 2013;Vogel et al., 2015;Yan and Bian, 2015). Chen et al. (2012) investigated air mass boundary layer sources and stratospheric entrainment regions based on a climatological
120 domain-filling Lagrangian study in the Asian summer monsoon area. The West Pacific Ocean

and the Bay of Bengal are found to be important source regions, while maximum stratospheric entrainment occurred above the tropical West Indian Ocean.

The Asian monsoon circulation could be an important pathway for the stratospheric entrainment of oceanic VSLS (Hossaini et al., 2016), because the steady southwest monsoon winds in the lower troposphere during boreal summer deliver oceanic air masses from the tropical Indian Ocean towards India and the Bay of Bengal (Lawrence and Lelieveld, 2010), where they are lifted by the monsoon convection and the Asian monsoon anticyclone. However, little is known about the emission strength of VSLS from the Indian Ocean and their transport pathways. A few measurements in the Bay of Bengal (Yamamoto et al., 2001) and Arabian Sea (Roy et al., 2011) as well as global source estimates suggest that the Indian Ocean might be a considerable source (Liang et al., 2010; Ziska et al., 2013). No bromocarbon data is available for the equatorial and southern Indian Ocean, yet, but CH_3I , which has been measured around the Mascarene Plateau, showed high oceanic concentrations (Smythe-Wright et al., 2005). Liang et al. (2014) use a Chemistry Climate Model for the years 1960 to 2010 and ~~project-modeled~~ that the tropical Indian Ocean delivers more bromine to the stratosphere than the tropical Pacific because of its higher atmospheric surface concentrations based on the global top-down emission estimate by Liang et al. (2010).

In this study, we show surface ocean concentrations and atmospheric mixing ratios of the halogenated VSLS CH_3I , and for the first time for CHBr_3 and CH_2Br_2 , in the subtropical and tropical West Indian Ocean during the Asian summer monsoon. We use the Lagrangian transport model Flexpart to investigate the atmospheric transport pathways of observation-based oceanic VSLS emissions to the stratosphere.

Our questions for this study are: Is the tropical Indian Ocean a source for atmospheric VSLS? What is the transport pathway from the West Indian Ocean to the stratosphere during the Asian summer monsoon? How much VSLS are delivered from the West Indian Ocean to the stratosphere during Asian summer monsoon? How large is the interannual variability of this VSLS entrainment?

In Sect. 2, we describe the cruise data and the transport model simulations. In Sect. 3, the results from the cruise measurements and trajectory calculations are shown and discussed. Then the spatial and interannual variability of transport is presented in Sect. 4. In Sect. 5, we address uncertainties before summarizing the results and concluding in Sect 6.

2 Data and Methods

2.1 Observations during the cruise

155 During two consecutive research cruises in the West Indian Ocean, we observed meteorological, oceanographic, and biogeochemical conditions, including atmospheric mixing ratios and oceanic concentrations of halogenated VSLs. The two cruises on RV *Sonne*, SO234-2 from July 08 to 19, 2014 (Durban, South Africa - Port Louis, Mauritius) and SO235 from July 23 to August 7, 2014 (Port Louis, Mauritius - Malé, Maldives), were conducted within the SPACES (Science
160 Partnerships for the Assessment of Complex Earth System Processes) and OASIS (Organic very short lived Substances and their air sea exchange from the Indian Ocean to the Stratosphere) research projects. Cruise SO234-2 was an international training and capacity building program for students from Germany and South African countries, whereas SO235 was purely scientifically oriented. The cruise tracks covered subtropical waters, coastal and shelf areas, and
165 the tropical open West Indian Ocean, and were designed to cover biologically productive and non-productive regions (Fig. 1). In the following, we will refer to the combined cruises as the “OASIS cruise”.

We collected meteorological data from ship based sensors including surface air temperature (SAT), relative humidity, air pressure, wind speed and direction taken every second
170 at about 25 m height on RV *Sonne*. Sea surface temperature (SST) and salinity (SSS) were measured in the ship’s hydrographic shaft at 5 m depth. We averaged all parameters to 10 minute intervals for our investigations.

During the cruise, we launched 95 radiosondes and thus obtained high resolution atmospheric profiles of temperature, wind, and humidity. During the first half of the cruise,
175 regular radiosondes were launched at 0 and 12 UTC, and additionally at 6 and 18 UTC during the 48 hour station (June 16 -18, 2014; Fig. 1). During the second half of the cruise, the launches were always performed at standard UTC times (0, 6, 12, 18 UTC), and every three hours during the diurnal stations (June 26 and 28, Aug. 3, 2014). For the regular launches, we used GRAW DFM-09 radiosondes and for the six ozone sonde launches we used DFM-97. The collected
180 radiosonde data was delivered in near real time to the Global Telecommunication System (GTS) to improve meteorological reanalyses (e.g. European Centre for Medium-Range Weather Forecasts (ECMWF) Re-Analysis Interim (ERA-Interim)) and operational forecast models (e.g. opECMWF (operational ECMWF)) in the subtropical and tropical West Indian Ocean.

Trace gas emissions are generally well mixed within the marine atmospheric boundary layer (MABL) on timescales of an hour or less by convection and turbulence (Stull, 1988). We determined the stable layer that defines the top of the MABL with the practical approach described in Seibert et al. (2000). From the radiosonde ascent we computed the vertical gradient of virtual potential temperature, which indicates the stable layer at the top of the MABL with positive values. A detailed description of our method can be found in Fuhlbrügge et al. (2013).

We collected a total of 213 air samples with a 3-hourly resolution at about 20 m height above sea level. These samples were pressurized to 2 atm in pre-cleaned stainless steel canisters with a metal bellows pump, and they were analyzed within 6 months after the cruise. Details about the analysis, the instrumental precision, the preparation of the samples, and the use of standard gases are described in Schauffler et al. (1999), Montzka et al. (2003), and Fuhlbrügge et al. (2013).

We collected overall 154 water samples spaced about every three hours from the hydrographic shaft of RV *Sonne* at a depth of 5 m. The samples were then analyzed for halogenated compounds using a purge and trap system onboard, attached to a gas chromatograph with electron capture detector. Analytical reproducibility of 10 % was determined from measuring duplicate water samples. Calibration was performed with a liquid mixed-compound standard prepared in methanol. Details of the procedure can be found in Hepach et al. (2016).

The sea-air flux (F) of the VSLS was calculated from the transfer coefficient (k_w) and the concentration gradient (Δc) according to Eq. (1). The gradient is between the water concentration (c_w) and theoretical equilibrium water concentration (c_{atm}/H), which is derived from the atmospheric concentration (c_{atm}). We use Henry's law constants (H) of Moore and coworkers (Moore et al., 1995a; Moore et al., 1995b).

$$F = k_w \cdot \Delta c = k_w \cdot \left(c_w - \frac{c_{\text{atm}}}{H} \right) \quad (1)$$

Compound-specific transfer coefficients were determined using the air-sea gas exchange parameterization of Nightingale et al. (2000) and applying a Schmidt number (Sc) for the different compounds as in Quack and Wallace (2003) (Eq. (2)).

$$k_w = k \cdot \frac{Sc^{-\frac{1}{2}}}{600} \quad (2)$$

Nightingale et al. (2000) determined the transfer coefficient (k) as a function of the wind speed at 10 m height (u_{10}): $k = 0.2 u_{10}^2 + 0.3 u_{10}$. This wind speed is derived from a logarithmic

wind profile using the von Kármán constant ($\kappa = 0.41$), the neutral drag coefficient (C_d) from Garratt (1977), and the 10 min average of the wind speed ($u(z)$) measured at $z = 25$ m during the cruise (Eq. (3)):

$$u_{10} = u(z) \frac{\kappa \sqrt{C_d}}{\kappa \sqrt{C_d} + \log \frac{z}{10}} \quad (3)$$

215

2.2 Trajectory calculations

For our trajectory calculations, we use the Lagrangian particle dispersion model Flexpart of the Norwegian Institute for Air Research in the Department of Atmospheric and Climate Research (Stohl et al., 2005), which has been evaluated in previous studies (Stohl et al., 1998;Stohl and Trickl, 1999). The model includes moist convection and turbulence parameterizations in the atmospheric boundary layer and free troposphere (Stohl and Thomson, 1999;Forster et al., 2007). In this study, we employ the most recently released version 9.2 of Flexpart. We use the ECMWF reanalysis product ERA-Interim (Dee et al., 2011) with a horizontal resolution of $1^\circ \times 1^\circ$ and 60 vertical model levels as meteorological input fields, providing air temperature, winds, boundary layer height, specific humidity, as well as convective and large scale precipitation with a 6-hourly temporal resolution. The vertical winds in hybrid coordinates were calculated mass-consistently from spectral data by the pre-processor (Stohl et al., 2005). We record the transport model output every 6 hours.

We ran the Flexpart model with three different setups, which are described in Table 1. These configurations are designated as 1) *OASIS backward* trajectories, 2) *OASIS* (forward trajectories), and 3) *Indian Ocean* (regional forward trajectories).

We calculate *OASIS backward* trajectories from the 12 UTC locations of RV *Sonne* during the cruise. These trajectories are later used to determine the source regions of air masses investigated along the cruise track.

With the *OASIS* setup, we study the transport of oceanic CHBr_3 , CH_2Br_2 , and CH_3I emissions from the measurement locations into the stratosphere similar as was carried out in the corresponding study by Tegtmeier et al. (2012). At every position along the cruise track at which emissions were calculated (Section 2.1), we release a mass of the compound equal to a release from $0.0002^\circ \times 0.0002^\circ$ in one hour. The mass is evenly distributed among 10,000 trajectories. During transport, CHBr_3 and CH_2Br_2 mass is depleted according to atmospheric lifetime profiles from Hossaini et al. (2010) based on Chemistry Transport Model simulations including VLSL

240

chemistry. CH₃I decays applying a uniform vertical lifetime of 3.5 days (Sect. 1). The mass on all trajectories that reach a height of 17 km is summed and assumed to be entrained into the stratosphere. This threshold height represents the average cold point tropopause (CPT) height during the cruise (see Fig. S2) and also for the whole tropics (Munchak and Pan, 2014). The influence of the entrainment height criteria is further discussed in Sect. 4. For intercomparison with other ocean basins, we employed exactly the same model-setup of transport simulations (including lifetimes) and the same emission calculation method for three previous corresponding cruises in the tropics: the TransBrom campaign in the West Pacific in 2009 (Introduction to special issue: Krüger and Quack, 2013), the SHIVA campaign in the South China and Sulu Seas in 2011 (Fuhlbrügge et al., 2016a), and the MSM18/3 cruise in the equatorial Atlantic Cold Tongue (Hepach et al., 2015).

The transport calculations based on the measured emissions from OASIS give insight into the contribution of oceanic emissions to the stratosphere during Asian summer monsoon. However, transport and emissions in the *OASIS* study are localized in space and time, and could thus be very different for different areas and years. In order to investigate the transport from the West Indian Ocean basin to the stratosphere and its interannual variability under the influence of the Asian summer monsoon circulation (*Indian Ocean* setup), we calculate trajectories from a large region of the tropical West Indian Ocean surface for the years 2000-2015. Trajectories are uniformly started within the release area (50°E-80°E, 20°S-10°N), covering the tropical West Indian Ocean, once every day during the month July in 2000-2015. The run time is set to 3 months, which covers the period July to October. We then calculate the fraction (q) of each *VLSL* tracer that reaches the stratosphere during the transit time (tt) assuming an exponential decay of the tracer (Eq. 4) according to the tropical tropospheric lifetimes (lt) of 17, 150, and 3.5 days for CHBr₃, CH₂Br₂, and CH₃I, respectively (Carpenter et al., 2014).

$$q = e^{-\frac{tt}{lt}} \quad (4)$$

We use the term “VLSL tracer” to distinguish from the calculations used in the *OASIS* setup, where actual VLSL emissions experience decay according to a vertical lifetime profile (uniform for CH₃I). The use of VLSL tracers allows us to evaluate one model run for different compounds with varying lifetimes. This *Indian Ocean* setup provides information on the preferred pathways from the West Indian Ocean to the stratosphere for different transport timescales and on their interannual variability. This variability is quantified by the coefficient of

variation (CV), which is defined as the ratio of the standard deviation to the mean entrainment. The correlations of the interannual variations between different regions of stratospheric entrainment are given by the correlation coefficient (r) by Pearson (1895). We calculated the p-value to determine the 95% significance level of the correlations.

3 The Indian Ocean cruise: OASIS

3.1 Atmospheric circulation

SST and SAT during the OASIS cruise generally increase from south towards the equator (Fig. 2a). The SST is on average 1.5 °C higher than the SAT, which benefits convection. Minimum SSTs of 18 °C were measured from July 14 to 17, 2014 in the open subtropical Indian Ocean (30° S, 59° E) and maximum SSTs of 29 °C were measured around the equator.

The overall mean wind speed was 8.1 m s⁻¹, with lower wind speeds in the subtropics and close to the equator (5 m s⁻¹), and higher wind speeds (up to 15 m s⁻¹) in the trade wind region (July 23 to August 5, 20° - 5° S) (Fig. 2b). The mean wind direction during the cruise was southeast. While the wind direction showed large variability in the subtropics, southeasterly trade winds dominated between Mauritius and the equator. North of the equator the wind direction changed to westerly winds. Our in situ ship wind measurements deviate from the mean July wind field from ERA-Interim during the first part of the cruise south of Mauritius (Fig. 1a) due to the influence of a developing low pressure system (not shown). The steady trade winds during the second part of the cruise are well reflected in the July mean wind field from ERA-Interim. Surface winds from in situ ship measurements, radiosondes and time varying ERA-Interim data show good agreement (Fig. S1).

Air masses sampled during the cruise originate mainly from the open ocean (Fig. 3a). Trajectories started between South Africa and Mauritius generally come from the south. An influence of terrestrial sources is possible close to South Africa and Madagascar. From Mauritius to the Maldives, the trajectories originate from the southeast open Indian Ocean. The analysis of air samples reveal no recent fresh anthropogenic input, indicated by the very low levels of short-lived trace gas contaminants, e.g. butane (lifetime 2.5 days; Finlayson-Pitts and Pitts, 2000), in this region (not shown).

3.2 VLSL observations and oceanic emissions

CHBr₃, CH₂Br₂, and CH₃I surface ocean concentrations, atmospheric mixing ratios, and emissions for the OASIS cruise are plotted as time series in Fig. 2c-e, and are summarized in
305 Table 2.

CHBr₃ concentrations in the surface ocean range from 1.3 to 33.4 pmol L⁻¹ with an average over all measurements of 8.4 ± 14.2 (1 σ) pmol L⁻¹. The standard deviation (σ) is used as a measure of the variability in the measurements during the cruise. We measured ~~higher-large~~
water concentrations of >10 pmol L⁻¹ close to coasts and shelf regions and in the open Indian
310 Ocean between 5° and 10° S (July 27- Aug. 2). Oceanic concentrations of CH₂Br₂ are
~~lowersmaller~~, with a mean of 6.7 ± 12.6 pmol L⁻¹, but show a similar pattern to CHBr₃
concentrations. High concentrations were measured southeast of Madagascar, when we passed
the southern stretch of the East Madagascar Current. Oceanic upwelling occurs along the eddy-
rich, shallow region south of Madagascar, which leads to locally enhanced phytoplankton growth
315 (Quarty et al., 2006), and possibly upwelling of elevated CH₂Br₂ concentrations from the deeper
ocean could have occurred similar as was observed for the equatorial upwelling in the Atlantic
(Hepach et al., 2015). CH₃I oceanic concentrations range from 0.2 to 16.4 pmol L⁻¹ with a mean
of 3.4 ± 3.1 pmol L⁻¹. They were elevated (5-12 pmol L⁻¹) during the last part of the cruise
(Aug. 3-6, 2014) around the equator. In the region of the Mascarene Plateau, to the west of our
320 cruise, Smythe-Wright et al. (2005) detected much ~~higher-larger~~ CH₃I concentrations between 20
and 40 pmol L⁻¹ during June-July 2002.

Atmospheric mixing ratios CHBr₃ during the OASIS cruise (Fig. 2d, Table 2) show an overall mean of 1.20 ± 0.35 ppt. Elevated mixing ratios of >2 ppt are found in three locations: south of Madagascar, in Port Louis, and close to the British Indian Ocean Territory. The first two
325 have probably terrestrial or coastal sources, because they do not coincide with high oceanic
CHBr₃ concentrations but backward trajectories pass land. Close to the British Indian Ocean
Territory, oceanic concentrations and atmospheric mixing ratios are elevated, which suggests a
local oceanic source. Atmospheric mixing ratios of CH₂Br₂ vary little around the average of
0.91 ppt and show a similar pattern as the CHBr₃ mixing ratios. CH₃I (0.84 ± 0.12 ppt) mixing
330 ratios show pronounced variations and surpass 1 ppt in some locations. These atmospheric
mixing ratios above the open ocean are much lower than the average of 12 pptv Smythe-Wright
et al. (2005) reported around the Mascarene Plateau.

We calculated oceanic emissions from the synchronized measurements of surface water
concentration and atmospheric mixing ratio as described in Section 2.1 (Fig. 2e and Fig 1). ~~High~~

335 | Strong emissions are caused by high oceanic concentrations, high wind speeds, or a combination
of both. The OASIS emission strength of CHBr_3 ranges from -100 to $9630 \text{ pmol m}^{-2} \text{ hr}^{-1}$ with
high mean emissions of $910 \pm 1,160 \text{ pmol m}^{-2} \text{ hr}^{-1}$, caused by moderate water concentrations and
relatively high wind speeds. We derive the highest-strongest emissions south of Madagascar and
in the trade wind regime from 5° S to 10° S above the open ocean upwelling region of the
340 Seychelles-Chagos-thermocline ridge (Schott et al., 2009), where we also observed enhanced
phytoplankton growth (not shown here). CH_2Br_2 emissions (with an overall mean of
 $930 \pm 2,000 \text{ pmol m}^{-2} \text{ hr}^{-1}$) were by far highest-strongest south of Madagascar with a single
maximum of up to $20,000 \text{ pmol m}^{-2} \text{ hr}^{-1}$. Here, we experienced very high oceanic concentrations
and high wind speeds due to the passage of a low pressure system south of the ship track during
345 July 11-17, 2014. CH_3I emissions ($460 \pm 430 \text{ pmol m}^{-2} \text{ hr}^{-1}$) had a pronounced maximum of
 $2,090 \text{ pmol m}^{-2} \text{ hr}^{-1}$ around 10° S and 70° E (July 31- Aug. 1), in accordance with high wind
speeds and oceanic concentrations being elevated close to the above mentioned open ocean
upwelling observed between 5° and 10° S .

During the first part of the cruise, we recorded low mean atmospheric mixing ratios of
350 CHBr_3 and CH_2Br_2 , despite high local oceanic concentrations and emissions especially south of
Madagascar. In connection with a high and well ventilated MABL (Fig. S2), this indicates that
the strong sources south of Madagascar are highly localized. The occasional enhancement of the
brominated VSLs in some air samples underlines the patchiness of the sources in this region.
During the second part of the cruise, the atmospheric mixing ratios of CHBr_3 and CH_2Br_2
355 increased from south to north and in the direction of the wind maximizing close to the equator
(Fig. 2d). The emissions were high-strong between Mauritius and the equator (Fig. 2e). This
suggests that the air around the equator was enriched by the advection of the oceanic emissions
with the trade winds from south to north. We assume that the bromocarbons accumulate because
of the steady wind directions and the suppression of mixing into the free troposphere by the top
360 of the MABL and the trade inversion layer (Fig. S2, July 27- Aug. 2) acting as strong transport
barriers for VSLs as was observed for the Peruvian upwelling (Fuhlbrügge et al., 2016a).

3.3 Comparison of OASIS VSLs emissions with other oceanic regions

Average emissions of the three VSLs from OASIS and other tropical cruises and modeling
365 studies are summarized in Table 3. We compare with cruises and open ocean estimates, since

OASIS mainly covered open ocean regions and only small coastal areas close to Madagascar, the British Indian Ocean Territory and the Maldives.

The average CHBr_3 emission during the OASIS campaign ($910 \text{ pmol m}^{-2} \text{ hr}^{-1}$) was ~~higher~~ larger than during most campaigns in tropical regions: 1.5 times ~~higher-larger~~ than during TransBrom in the subtropical and tropical West Pacific (Tegtmeier et al., 2012), 1.2 times ~~higher~~ larger than during DRIVE in the tropical North East Atlantic (Hepach et al., 2014), and 1.5 times ~~higher-larger~~ than during MSM18/3 in the Atlantic equatorial upwelling (Hepach et al., 2015). Only the SHIVA campaign in the South China and Sulu Seas yielded ~~higher-larger~~ CHBr_3 emissions of $1,486 \text{ pmol m}^{-2} \text{ hr}^{-1}$ because of very high oceanic concentrations close to the coast (Fuhlbrügge et al., 2016b). The global open ocean estimate by Quack and Wallace (2003) is one-third ~~lower-smaller~~ than our measured values in the West Indian Ocean. The bottom-up emission climatology by Ziska et al. (2013) estimates ~~lower-smaller~~ values for the Indian Ocean, based on measurements from other oceanic basins due to a lack of available Indian Ocean in situ measurements. With their top-down approach, Warwick et al. (2006), Liang et al. (2010), and Ordóñez et al. (2012) calculated CHBr_3 emissions in the range of $580\text{-}956 \text{ pmol m}^{-2} \text{ hr}^{-1}$ for the tropical ocean. Stemmler et al. (2014) modeled very low CHBr_3 emissions around $200 \text{ pmol m}^{-2} \text{ hr}^{-1}$ for the equatorial Indian Ocean with their biogeochemical ocean model.

Average CH_2Br_2 emissions from the OASIS cruise ($930 \text{ pmol m}^{-2} \text{ hr}^{-1}$) are 2-6 times ~~higher-larger~~ than average cruise emissions listed in Table 3: TransBrom, DRIVE, MSM18/3, SHIVA, and M91. This is caused by the generally high oceanic concentrations during OASIS, with ~~highest-largest~~ values south of Madagascar. The mean emissions from the West Indian Ocean are also much ~~higher-stronger~~ than the tropical ocean estimate from Butler et al. (2007), and the global open ocean estimate from Yokouchi et al. (2008) and Carpenter et al. (2009). The top-down model approach by Liang et al. (2010) yielded the ~~lowest-weakest~~ emissions of only $81 \text{ pmol m}^{-2} \text{ hr}^{-1}$. The Ziska et al. (2013) climatology shows maximum equatorial Indian Ocean CH_2Br_2 emission values around $500 \text{ pmol m}^{-2} \text{ hr}^{-1}$.

The average CH_3I emissions during OASIS ($460 \text{ pmol m}^{-2} \text{ hr}^{-1}$) were in the range of previously observed and estimated values from 254 to $625 \text{ pmol m}^{-2} \text{ hr}^{-1}$ (Table 3). Only for the highly productive Peruvian Upwelling, Hepach et al. (2016) calculated much ~~higher-larger~~ emissions of $954 \text{ pmol m}^{-2} \text{ hr}^{-1}$. The coupled ocean-atmosphere model of Bell et al. (2002) produced average global emissions of $670 \text{ pmol m}^{-2} \text{ hr}^{-1}$, while Stemmler et al. (2013) modeled CH_3I emissions around $500 \text{ pmol m}^{-2} \text{ hr}^{-1}$ for the tropical Atlantic with their biogeochemical

ocean model. The Ziska et al. (2013) climatology shows Indian Ocean CH₃I emissions around 500 pmol m⁻² hr⁻¹.

In general, the emissions during the OASIS cruise in the subtropical and tropical West Indian Ocean were as strong as or stronger than in other tropical open ocean cruises or studies. Especially CH₂Br₂ emissions during the OASIS cruise were stronger than any previous emission estimates. The West Indian Ocean seems to be a region with significant contribution to the global open ocean VSLs emissions, especially in boreal summer when wind speeds are high because of the southwest monsoon circulation.

3.4 VSLs entrainment to the stratosphere during OASIS

The OASIS forward trajectories released at the locations of the VSLs measurements show the transport pathway of the air masses from their sample points along the cruise track (Fig. 3b). The mean of all 10,000 trajectories from each release can be grouped into four regimes according to transport direction: Westerlies, Transition, Monsoon Circulation, and Local Convection. The air masses in the Westerlies regime are transported to the Southeast Indian Ocean and the air masses from the Transition regime propagate towards Madagascar and Africa. Flexpart calculations reveal that both transport regimes lift air masses up to a mean height of about 5.3 km after one month (not shown here). The trajectories of the Monsoon Circulation regime first travel with the southeasterly trade winds and then with the southwesterly monsoon winds. The trajectories stay relatively close to the ocean surface (below 3 km) until they reach the Bay of Bengal, where they are rapidly lifted to the upper troposphere. On average they reach a height of 7.9 km after one month, which reveals that this is the regime with most convection. The trajectories of the Local Convection regime mainly experience rapid uplift around the equator. After one month this group has reached a mean height of 7.2 km. The different uplifts are reflected in the vertical distribution of bromoform in each transport regime (Fig. S2).

The absolute entrainment of oceanic VSLs to the stratosphere depends on the emission strength as well as the *transport efficiency* (Fig. 4). This efficiency is defined as the ratio between entrained and emitted VSLs. It depends on the *transit time*, defined as the time an air parcel needs to be transported from the ocean surface to 17 km height, and the lifetime of the compound. For stratospheric entrainment the transit time must be in the order of the lifetime of a compound or shorter. If the transit time is considerably larger than the lifetime, most of the compound has decayed before reaching the stratosphere. In the following, we will use the expressions VSLs

430 *transit time*, which is the transit time including loss processes of the VSLs in the atmosphere
during the transport, and *transit half-life*, which is the time after which half of the total amount of
entrained tracer compound has reached-been entrained above 17 km. We also calculated the
relative emission and entrainment by regime. Table 4 displays the absolute and relative emissions
and entrainment, the transport efficiency, and the transit half-life for the whole cruise and the four
435 regimes.

The mean sea surface release of CHBr_3 in Flexpart is $0.43 \mu\text{mol}$ (on $0.0002^\circ \times 0.0002^\circ \text{ hr}^{-1}$) during the cruise and the mean entrainment to the stratosphere is 5.5 nmol resulting
in a mean transport efficiency of 1.3 %. CH_2Br_2 has a higher transport efficiency of 6.45.5 %
with mean emissions of $0.43 \mu\text{mol}$ (on $0.0002^\circ \times 0.0002^\circ \text{ hr}^{-1}$), and very high stratospheric
440 entrainment of 23.6 nmol . CH_3I has a low transport efficiency of 0.3 % with mean emissions of
 $0.22 \mu\text{mol}$ (on $0.0002^\circ \times 0.0002^\circ \text{ hr}^{-1}$) and stratospheric entrainment of 0.7 nmol .

The four transport regimes show different transport efficiencies of CHBr_3 , CH_2Br_2 , and
 CH_3I to the stratosphere. The two most efficient regimes, transporting CHBr_3 and CH_3I to the
stratosphere during the OASIS cruise, were the Monsoon Circulation and the Local Convection
445 regime.

The transport efficiency for all three compounds is highest in the Local Convection
regime ($\text{CHBr}_3 \sim 3$ %, $\text{CH}_2\text{Br}_2 \sim 9$ %, and $\text{CH}_3\text{I} \sim 1$ %), because this regime has the shortest transit
half-life for all three VSLs. For CH_3I , the compound with the shortest lifetime, the fast transport
plays the largest role, and thus this regime is by far the most efficient.

450 For CHBr_3 , the regime with most absolute and relative stratospheric entrainment (11 nmol ,
 57 %) is the Monsoon Circulation regime, because of the high emissions in the source region and
the high transport efficiency. Although the CHBr_3 emissions are as high in the Westerlies regime,
the entrainment is small (2 nmol , 9 %), because of a low transport efficiency due to slow
transport visible in the long transit half-life. The Local Convection regime has the highest
455 transport efficiency, but emissions were low, resulting in less entrainment (4 nmol , 23 %) than in
the Monsoon Circulation regime. The absolute entrainment of CH_2Br_2 strongly depends on the
strength of emission, because the transport efficiency is relatively similar for all transport regimes
due to the long lifetime of the compound. Most entrained CH_2Br_2 comes from the Westerlies
regime (29 nmol , 35 %), where sources especially south of Madagascar were extremely strong.
460 Although these emissions occur in the subtropics, they reach 17 km mainly in the tropics (Fig.
S3). The transport efficiency of 4 % still allows a large amount of 345 nmol CH_2Br_2 to enter the

stratosphere from the maximum emissions at 23 UTC on July 12, 2014 (Fig. 4). CH₃I absolute entrainment (2.8 nmol, 79 %) is highest in the Local Convection regime, because of both highest emissions and highest transport efficiency (Table 4).

465

3.5 Comparison of VLSL entrainment to the stratosphere with other oceanic regions

A comparison of the subtropical and tropical Indian Ocean contribution to the stratosphere with other tropical ocean regions, applying the same emission calculation and model-setup (Sect. 2.2) for CHBr₃ is shown in Table 5. Though the Western Pacific TransBrom cruise had lower bromoform emission rates compared to OASIS, stratospheric entrainment was greater for the Western Pacific region compared to the Indian Ocean. This difference was caused by a higher transport efficiency of 4.4 % in the West Pacific influenced by tropical cyclone activity in October 2009 (Krüger and Quack, 2013). Tegtmeier et al. (2012) obtained a higher transport efficiency of 5 % for TransBrom using a previous Flexpart model (version 8.0). During the SHIVA campaign in the South China Sea, high oceanic concentrations of bromoform produced mean emission rates that were higher than during OASIS. The SHIVA calculations show even higher transport efficiencies of 7.9 %, which lead to an entrainment of 48.4 nmol CHBr₃ (Table 5), because of the strong convective activity in that region during the time (Fuhlbrügge et al., 2016b). The MSM18/3 cruise in the equatorial Atlantic (Hepach et al., 2015) has the smallest emissions, entrainment, and a transport efficiency of 0.8 % (Table 5). Overall, the comparison indicates that more CHBr₃ was entrained to the stratosphere from the tropical West Pacific than from the tropical West Indian Ocean during Asian summer monsoon, using available in situ emissions and 6-hourly meteorological fields. This is in contrast to the study by Liang et al. (2014), who ~~projected~~determined with a chemistry climate model climatology that emissions from the tropical Indian Ocean deliver more brominated VLSL into the stratosphere than tropical West Pacific emissions.

CH₂Br₂ entrainment to the stratosphere for the TransBrom ship campaign was ~8 nmol with transport efficiencies of 15 % (Tegtmeier et al., 2012). This is much higher than the Indian Ocean transport efficiency of 6.4 %, but the absolute entrainment of 23.6 nmol CH₂Br₂ we calculated for the OASIS cruise (Table 4) is much higher than during TransBrom, because of the very strong CH₂Br₂ emissions during OASIS.

495 Tegtmeier et al. (2013) investigated CH₃I entrainment to the stratosphere for three tropical ship campaigns: SHIVA and TransBrom in the tropical West Pacific, and DRIVE in the tropical North East Atlantic. They used a CH₃I lifetime profile between 2-3 days. The transport efficiencies were 4 %, 1 %, and 0.1 %, respectively. The OASIS Indian Ocean mean transport efficiency for CH₃I (0.3 %, Table 4), applying a uniform lifetime profile of 3.5 days, is lower than in the West Pacific, but higher than in the Atlantic.

500 Uncertainties of VSLs emissions and modeling their transport to the stratosphere will be further discussed in Sect. 5.

4 General transport from West Indian Ocean to the stratosphere

4.1 Spatial variability of stratospheric entrainment

505 We calculate the entrainment at 17 km for CHBr₃, CH₂Br₂, and CH₃I tracers by weighting the trajectories from the West Indian Ocean release region for July 2000-2015 with the transit-time-dependent atmospheric decay plotted in Fig. 5. A summary of transport efficiency, transit half-life, and entrainment correlations for all three VSLs can be found in Table 6.

510 The distribution of VSLs transit times shows that the shorter the lifetime of a compound, the more important is the transport on short timescales (Fig. 5). For CHBr₃, CH₂Br₂, and CH₃I tracers the transit half-lives are 8.5, 27.2, and 1.9 days, respectively (Table 6). For the two bromocarbons, the transit time distribution shows two maxima, one for the 0-2 days bin, and the second between 4-10 days for CHBr₃ and 6-12 days for CH₂Br₂. CH₃I tracer entrainment occurs mainly on timescales up to 2 days (Fig. 5).

515 The stratospheric entrainment regions during Asian summer monsoon between 2000 and 2015 are displayed at the locations where the trajectories first reach 17 km (Fig. 6). The VSLs tracers show two main entrainment regions. Enhanced entrainment occurs above Bay of Bengal and northern India in the southeastern part of the Asian monsoon anticyclone, and is connected to the Monsoon Circulation transport regime (Sect. 3.4). The second entrainment region is above the tropical West Indian Ocean, and belongs to the Local Convection regime. We define these two
520 regions to enclose the core entrainment and to be evenly sized in grid space (colored boxes in Fig. 6).

The larger West Indian Ocean release area and longer time series analysis (Table 6) confirms the results of our OASIS analysis (Table 4). The longer-lived VSLs tracers (CHBr₃ and

525 CH₂Br₂) are mainly entrained through the Monsoon Circulation regime, while the Local Convection regime is more important for the shortest-lived tracer (CH₃I).

Chen et al. (2012) also identified these two stratospheric entrainment regions, analyzing the air transport from the atmospheric boundary layer to the tropopause layer in the Asian Summer monsoon region for a 9 year climatology. Additionally, they registered entrainment over the West Pacific Ocean, but the Local Convection entrainment above the central Indian Ocean was by far the strongest. Similar to our VLSL transit times, the study of Chen et al. (2012) found very short transport timescales of 0-1 days in the equatorial West Indian Ocean, while transit times above the Bay of Bengal and northern India were between 3 and 9 days.

535 4.2 Interannual variability of stratospheric entrainment

The time series of stratospheric entrainment from the West Indian Ocean to the stratosphere shows interannual variability for all three VLSL tracers (Fig. 7). Overall, July 2014 revealed high entrainment for CHBr₃ and CH₂Br₂ tracers and low entrainment for CH₃I tracer. The coefficient of variation (CV) for total entrainment is 0.13, 0.09, and 0.21 for CHBr₃, CH₂Br₂ and CH₃I, respectively. Thus, the shortest-lived compound CH₃I has the strongest interannual variation, the longest-lived CH₂Br₂ the weakest variation.

In order to analyze which transport regime has a stronger influence on the total entrainment variability, we correlated the interannual entrainment time series of total entrainment with the entrainment in the Monsoon Circulation and Local Convection regimes (Table 6). Interannual variability of CHBr₃ and CH₂Br₂ tracer entrainment results mainly from variability in the Monsoon Circulation regime ($r = 0.54$ and $r = 0.56$, respectively). In contrast, the interannual variability of CH₃I tracer entrainment is highly correlated with the Local Convection regime variability ($r = 0.8791$). The high variability of total CH₃I entrainment (CV = 0.21) implies that interannual variation in convection is larger than in the monsoon circulation. The interannual time series of Monsoon Circulation and Local Convection regime reveal a weak inverse correlation for all three compounds, suggesting that more entrainment in one regime is related to less entrainment in the other (Fig. 7).

The interannual time series of total VLSL tracer entrainment displays a small increase over time. This increase is independent of the chosen entrainment height (between 13 km and 19 km, Fig. S4), and is visible in the analysis for all three tracers. The increase is strongest for CHBr₃ and weaker for the other two compounds. It arises mainly from an increase of entrainment in the

Monsoon Circulation regime (Fig. 7). Analyzing changes of rainfall revealed an increase in precipitation over northeastern India for the time interval of our transport study (Latif et al., 2016;Preethi et al., 2016). This indicates an increase of convection in our Monsoon Circulation regime over the years from 2000 to 2015, which can explain the increase in stratospheric entrainment. However, for the long time period from the 1950s to the 2010s the same authors found a decrease of precipitation over the above mentioned area, potentially impacting the VLSL entrainment to the stratosphere.

In a follow-up study we will investigate the influence of the seasonal cycle of the Asian Monsoon circulation and interannual influences through atmospheric circulation patterns on the West Indian Ocean VLSL entrainment to the stratosphere in more detail.

5 Uncertainties in the analysis

This study confirms that the subtropical and tropical West Indian Ocean is a source region of oceanic halogenated VLSL to the stratosphere during the Asian summer monsoon. The amount of VLSL entrained depends on the emission strength, the lifetime of the compound, and the transport of trajectories in the regime, which have been quantified in this study.

However, uncertainties of this study are present in various aspects of the analysis. The uncertainties result from the calculation of VLSL emissions, the Flexpart transport using ERA-Interim reanalysis fields, and the definition of entrainment to the stratosphere.

The calculation of VLSL emissions from the concentration gradient between the ocean at 5 m depth and the atmosphere at 20 m height is subject to measurement uncertainties and a possible different concentration gradient directly at the air-sea interface. Also the applied wind-speed-based parameterization for air-sea flux, which represents a reasonable mean of the published parameterizations, is uncertain by more than a factor of two (Lennartz et al., 2015). Both factors may lead to a systematic flux under- or overestimation in our study.

A vital part of this study is the meteorological reanalysis data ERA-Interim and the Flexpart model for determining the VLSL transport. With delivery of our radiosonde launches to the GTS we have improved the data coverage over the Indian Ocean for the time of our study, and thus the quality of meteorological reanalysis. Indeed, horizontal wind speed and direction from ship sensors and sondes agree well with the ERA-Interim data (Fig. S1). As the scale of tropical convection is below the state of the art grid-scale of global atmospheric models it is not

sufficiently resolved and must be parameterized. The Lagrangian model Flexpart uses a convection scheme, described and evaluated by Forster et al. (2007), to account for vertical transport. Using Flexpart trajectories with ERA-Interim reanalysis, Fuhlbrügge et al. (2016b) were able to simulate VSLS mixing ratios from the surface to the free troposphere up to 11 km above the tropical West Pacific in very good agreement with corresponding aircraft measurements applying a simple source-loss approach. Tegtmeier et al. (2013) showed that Flexpart distribution of oceanic CH₃I in the tropics agrees well with adjacent upper tropospheric and lower stratospheric aircraft measurements, thus increasing our confidence in the Flexpart convection scheme and ERA-Interim velocities. Testing different Flexpart model versions (8.0 and 9.2) for stratospheric entrainment of CHBr₃ (not shown), has revealed only slightly lower stratospheric entrainment of 0.2 % with the more recent model version 9.2 used in this study here.

Another uncertainty in the location and variability of entrained trajectories may result from the definition of stratospheric entrainment (Sect. 2.2). For the tropics, the Cold Point Tropopause (CPT) is commonly used as boundary between the troposphere and the stratosphere (Carpenter et al., 2014). The average measured CPT height during OASIS was 17 km (Fig. S2), but it can be up to 17.6 km high within the Asian monsoon anticyclone during boreal summer season (Munchak and Pan, 2014). To test the sensitivity of our results with regard to the entrainment height, we analyzed entrained trajectories at several different tropical levels in the upper troposphere/lower stratosphere (UTLS) (13, 15, 17, and 18 km altitude, Fig. S4). As described in Sect. 3.4, we can follow the preferred transport pathways by the migration of maximum density at the intersecting UTLS levels. Analyzing the influence of applying different UTLS entrainment levels reveal an overall good agreement of interannual variability and long-term changes (Fig. S5).

6 Summary and conclusion

During the research cruise OASIS in the subtropical and tropical West Indian Ocean in July and August 2014, we conducted simultaneous measurements of the halogenated very short-lived substances (VSLS) methyl iodide (CH₃I), and for the first time of bromoform (CHBr₃) and dibromomethane (CH₂Br₂), in surface seawater and the marine atmosphere. Based on these measurements, we calculated high emissions of CHBr₃ of 910 ± 1160 pmol m⁻² hr⁻¹ caused by high oceanic concentrations south of Madagascar, and moderate concentrations combined with

high wind speeds (up to 15 ms^{-1}) in the trade wind regime above the open West Indian Ocean.
620 The average CHBr_3 emissions were at the higher end of previously reported values of the tropical
oceans. CH_2Br_2 emissions of $930 \pm 2,000 \text{ pmol m}^{-2} \text{ hr}^{-1}$ were especially high also south of
Madagascar, and on average higher than reported from cruises in other tropical regions, from
global observational and model based climatologies. CH_3I emissions ($460 \pm 430 \text{ pmol m}^{-2} \text{ hr}^{-1}$)
625 were highest around the equator, but in the range of previously reported emission rates from
subtropical and tropical ocean regions.

The stratospheric entrainment of these three VSLs from the West Indian Ocean during
Asian summer monsoon depends on the strength of emissions and the timescale of the transport
to the stratosphere in comparison to the lifetime of the compound. The entrainment of the
shortest-lived compound CH_3I (3.5 days) depends mainly on fast transport. The entrainment of
630 CH_2Br_2 strongly depends on the emission strength, because the transport efficiency is relatively
similar for all transport regimes due to the long lifetime of the compound (150 days). CHBr_3
(17 days lifetime) entrainment is influenced by both oceanic emissions and fast transport.

During the OASIS cruise we found four transport regimes with different VSLs emission
strengths and transport efficiencies. The Monsoon Circulation and the Local Convection regime
635 were most efficient for VSLs entrainment into the stratosphere. These two have different source
regions, VSLs transit times, stratospheric entrainment regions, and interannual variations
summarized in Fig. 8.

In the Monsoon Circulation regime, the oceanic VSLs transport pathway begins south of
the equator and follows the near surface winds to India and Bay of Bengal, where monsoon
640 convection rapidly lifts them into the upper troposphere. The VSLs ascend further within the
Asian monsoon anticyclone, being entrained to stratospheric levels in its southeastern part. The
transport to the stratosphere in this regime is effective for CHBr_3 and CH_2Br_2 (2 % and 8 %
transport efficiency, respectively), but less effective for CH_3I (0.3%) as its lifetime is shorter than
the transport timescale. Absolute CHBr_3 entrainment from the OASIS cruise was strongest in the
645 Monsoon Circulation regime because of strong emissions in the source region. The *Indian Ocean*
setup showed that it is generally the preferred regime for the entrainment of VSLs with longer
lifetimes during boreal summer, because many trajectories follow this transport pathway. Mean
transit half-lives from the West Indian Ocean surface to 17 km height are 6 days for CHBr_3 and
13 days for CH_2Br_2 .

650 In the Local Convection regime, VSLs are transported upwards by convection above the
tropical West Indian Ocean and entrained to the stratosphere in the vicinity of the equator. VSLs
transit times are short (0-2 days) and thus we found the highest transport efficiencies for CHBr_3 ,
 CH_2Br_2 , and CH_3I in this region (3 %, 9 %, and 1 %). The Local Convection regime is
responsible for most of the stratospheric entrainment of CH_3I from the OASIS cruise. The *Indian*
655 *Ocean* transport study supports this finding.

CH_2Br_2 transport efficiency is similar for all regimes of the OASIS cruise, because its
lifetime is longer than the transport timescale from ocean to stratosphere in the tropics. Absolute
entrainment of CH_2Br_2 thus strongly depends on the strength of emissions and these were very
high during OASIS, especially south of Madagascar.

660 In comparison to other corresponding cruises, the Monsoon Circulation and Local
Convection regime in the tropical West Indian Ocean show more entrainment of CHBr_3 and CH_3I
than the tropical Atlantic, but less than the tropical West Pacific Ocean. CH_2Br_2 entrainment from
the West Indian Ocean was higher than from previous corresponding cruises in other tropical
oceans due to the very high emissions.

665 A 16-year time series (2000-2015) of VSLs tracer entrainment from the West Indian Ocean
to the stratosphere through the monsoon circulation during July reveals strongest interannual
variability for CH_3I , the shortest-lived compound, which seems to be connected to the interannual
variation in convection above the West Indian Ocean. The weakest variations were found for
 CH_2Br_2 , the longest-lived compound, whose entrainment hardly depends on the local
670 atmospheric circulation. The time series of entrainment to the stratosphere shows an overall
increase for all three compounds, which is likely connected to a reported increase of precipitation
and convection over northeastern India during this time period. For CHBr_3 , whose transport is
mostly associated with the changing Asian summer monsoon circulation, the increase is stronger
than for the other two compounds.

675 Overall, the OASIS measurements confirm that during boreal summer the subtropical and
tropical West Indian Ocean is an important source for VSLs, especially of CH_2Br_2 , with
pronounced hot spots. This study demonstrates that the VSLs delivery from the West Indian
Ocean surface to the stratosphere depends on the regional strength of emissions and the transit
time in preferred transport regimes. Changes in the Asian summer monsoon circulation likely
680 impact the VSLs entrainment to the stratosphere.

Data availability

The underlying data will be available at the open-access library Pangaea (<http://www.pangaea.de>).

Author contribution

685 A. Fiehn, K. Krüger and B. Quack designed the experiments and A. Fiehn carried them out. All coauthors were involved in the VLSL measurements and analyses taken during the OASIS cruise. A. Fiehn, K. Krüger and B. Quack prepared the manuscript with contributions from all co-authors.

Competing interests

The authors declare that they have no conflict of interest.

Acknowledgements

690 This study was supported by BMBF grant SONNE 03G0235A. We acknowledge the authorities of Madagascar, Mauritius, the United Kingdom, and the Maldives for the permissions to work in their territorial waters. We would also like to thank the captain and crew of RV *Sonne* as well as the student participants during SPACES for their help and cooperation. We thank the European Centre for Medium-Range Weather Forecasts (ECMWF) for the provision of ERA-Interim
695 reanalysis data and the Flexpart development team for the Lagrangian particle dispersion model used in this publication. Part of the Flexpart simulations was performed on resources provided by UNINETT Sigma2 - the National Infrastructure for High Performance Computing and Data Storage in Norway. E. Atlas acknowledges support from NASA Upper Atmosphere Program Grant #NNX13AH20G.

700

References

- Bell, N., Hsu, L., Jacob, D. J., Schultz, M. G., Blake, D. R., Butler, J. H., King, D. B., Lobert, J. M., and Maier-Reimer, E.: Methyl iodide: Atmospheric budget and use as a tracer of marine convection in global models, *Journal of Geophysical Research: Atmospheres*, 107, ACH 8-1-ACH 8-12, 10.1029/2001jd001151, 2002.
- 705 Bergman, J. W., Fierli, F., Jensen, E. J., Honomichl, S., and Pan, L. L.: Boundary layer sources for the Asian anticyclone: Regional contributions to a vertical conduit, *Journal of Geophysical Research: Atmospheres*, 118, 2560-2575, 10.1002/jgrd.50142, 2013.

- 710 Butler, J. H., King, D. B., Lobert, J. M., Montzka, S. A., Yvon-Lewis, S. A., Hall, B. D., Warwick, N. J.,
Mondeel, D. J., Aydin, M., and Elkins, J. W.: Oceanic distributions and emissions of short-lived
halocarbons, *Global Biogeochemical Cycles*, 21, 10.1029/2006gb002732, 2007.
- 715 Carpenter, L. J., Sturges, W. T., Penkett, S. A., Liss, P. S., Alicke, B., Hebestreit, K., and Platt, U.: Short-lived
alkyl iodides and bromides at Mace Head, Ireland: Links to biogenic sources and halogen oxide
production, *Journal of Geophysical Research: Atmospheres*, 104, 1679-1689, 10.1029/98jd02746,
1999.
- Carpenter, L. J., Jones, C., Dunk, R., Hornsby, K., and Woeltjen, J.: Air-sea fluxes of biogenic bromine from
the tropical and North Atlantic Ocean, *Atmospheric Chemistry and Physics*, 9, 1805-1816, 2009.
- 720 Carpenter, L. J., Reimann, S., Burkholder, J. B., Clerbaux, C., Hall, B. D., Hossaini, R., Laube, J. C., and Yvon-
Lewis, S. A.: Ozone-Depleting Substances (ODSs) and other gases of interest to the Montreal
Protocol, in: *Scientific Assessment of Ozone Depletion: 2014. Global Ozone Research and
monitoring Project - Report N. 55*, World Meteorological Organization, Geneva, Switzerland,
2014.
- 725 Chen, B., Xu, X., Yang, S., and Zhao, T.: Climatological perspectives of air transport from atmospheric
boundary layer to tropopause layer over Asian monsoon regions during boreal summer inferred
from Lagrangian approach, *Atmospheric Chemistry and Physics*, 12, 5827-5839, 2012.
- 730 Dorf, M., Bösch, H., Butz, A., Camy-Peyret, C., Chipperfield, M. P., Engel, A., Goutail, F., Grunow, K.,
Hendrick, F., Hrechanyy, S., Naujokat, B., Pommereau, J. P., Van Roozendaal, M., Sioris, C., Stroh,
F., Weidner, F., and Pfeilsticker, K.: Balloon-borne stratospheric BrO measurements: comparison
with Envisat/SCIAMACHY BrO limb profiles, *Atmospheric Chemistry and Physics*, 6, 2483-2501,
10.5194/acp-6-2483-2006, 2006.
- Dvortsov, V. L., Geller, M. A., Solomon, S., Schauffler, S. M., Atlas, E. L., and Blake, D. R.: Rethinking
reactive halogen budgets in the midlatitude lower stratosphere, *Geophysical Research Letters*,
26, 1699-1702, 10.1029/1999gl900309, 1999.
- 735 Finlayson-Pitts, B., and Pitts, J.: *Chemistry of the upper and lower atmosphere: Theory, experiments and
applications*, Academic, US, 2000.
- Forster, C., Stohl, A., and Seibert, P.: Parameterization of convective transport in a Lagrangian particle
dispersion model and its evaluation, *Journal of Applied Meteorology and Climatology*, 46, 403-
422, 10.1175/JAM2470.1, 2007.
- 740 Fuhlbrügge, S., Krüger, K., Quack, B., Atlas, E., Hepach, H., and Ziska, F.: Impact of the marine
atmospheric boundary layer conditions on VLS abundances in the eastern tropical and
subtropical North Atlantic Ocean, *Atmospheric Chemistry and Physics*, 13, 6345-6357,
10.5194/acp-13-6345-2013, 2013.
- 745 Fuhlbrügge, S., Quack, B., Atlas, E., Fiehn, A., Hepach, H., and Krüger, K.: Meteorological constraints on
oceanic halocarbons above the Peruvian Upwelling, *Atmos. Chem. Phys. Discuss.*, 15, 20597-
20628, 10.5194/acpd-15-20597-2015, 2016a.
- Fuhlbrügge, S., Quack, B., Tegtmeier, S., Atlas, E., Hepach, H., Shi, Q., Raimund, S., and Krüger, K.: The
contribution of oceanic halocarbons to marine and free tropospheric air over the tropical West
Pacific, *Atmospheric Chemistry and Physics*, 16, 7569-7585, 10.5194/acp-16-7569-2016, 2016b.
- 750 Garratt, J. R.: Review of Drag Coefficients over Oceans and Continents, *Monthly Weather Review*, 105,
915-929, 10.1175/1520-0493(1977)105<0915%3ARODCOO>2.0.CO%3B2, 1977.

- Gettelman, A., Kinnison, D., Dunkerton, T. J., and Brasseur, G. P.: Impact of monsoon circulations on the upper troposphere and lower stratosphere, *Journal of Geophysical Research*, 109, 10.1029/2004jd004878, 2004.
- 755 Hense, I., and Quack, B.: Modelling the vertical distribution of bromoform in the upper water column of the tropical Atlantic Ocean, *Biogeosciences*, 6, 535-544, 10.5194/bg-6-535-2009, 2009.
- Hepach, H., Quack, B., Ziska, F., Fuhlbrügge, S., Atlas, E., Krüger, K., Peeken, I., and Wallace, D. W. R.: Drivers of diel and regional variations of halocarbon emissions from the tropical North East Atlantic, *Atmospheric Chemistry and Physics*, 14, 10.5194/acp-14-1255-2014, 2014.
- 760 Hepach, H., Quack, B., Raimund, S., Fischer, T., Atlas, E. L., and Bracher, A.: Halocarbon emissions and sources in the equatorial Atlantic Cold Tongue, *Biogeosciences*, 12, 6369-6387, 2015.
- Hepach, H., Quack, B., Tegtmeier, S., Engel, A., Bracher, A., Fuhlbrügge, S., Galgani, L., Atlas, E. L., Lampel, J., Frieß, U., and Krüger, K.: Biogenic halocarbons from the Peruvian upwelling region as tropospheric halogen source, *Atmospheric Chemistry and Physics*, 16, 12219-12237, 10.5194/acp-16-12219-2016, 2016.
- 765 Hoskins, B. J., and Rodwell, M. J.: A Model of the Asian Summer Monsoon. Part I: The Global Scale, *Journal of the Atmospheric Sciences*, 52, 1329-1340, 10.1175/1520-0469(1995)052<1329:AMOTAS>2.0.CO;2, 1995.
- 770 Hossaini, R., Chipperfield, M. P., Monge-Sanz, B. M., Richards, N. A. D., Atlas, E., and Blake, D. R.: Bromoform and dibromomethane in the tropics: a 3-D model study of chemistry and transport, *Atmospheric Chemistry and Physics*, 10, 2010.
- Hossaini, R., Chipperfield, M. P., Feng, W., Breider, T. J., Atlas, E., Montzka, S. A., Miller, B. R., Moore, F., and Elkins, J.: The contribution of natural and anthropogenic very short-lived species to stratospheric bromine, *Atmospheric Chemistry and Physics*, 12, 371-380, 10.5194/acp-12-371-2012, 2012.
- 775 Hossaini, R., Chipperfield, M. P., Montzka, S. A., Rap, A., Dhomse, S., and Feng, W.: Efficiency of short-lived halogens at influencing climate through depletion of stratospheric ozone, *Nature Geoscience*, 8, 186-190, 10.1038/ngeo2363, 2015.
- 780 Hossaini, R., Patra, P. K., Leeson, A. A., Krysztofiak, G., Abraham, N. L., Andrews, S. J., Archibald, A. T., Aschmann, J., Atlas, E. L., Belikov, D. A., Bönisch, H., Butler, R., Carpenter, L. J., Dhomse, S., Dorf, M., Engel, A., Feng, L., Feng, W., Fuhlbrügge, S., Griffiths, P. T., Harris, N. R. P., Hommel, R., Keber, T., Krüger, K., Lennartz, S. T., Maksyutov, S., Mantle, H., Mills, G. P., Miller, B., Montzka, S. A., Moore, F., Navarro, M. A., Oram, D. E., Palmer, P. I., Pfeilsticker, K., Pyle, J. A., Quack, B., Robinson, A. D., Saikawa, E., Saiz-Lopez, A., Sala, S., Sinnhuber, B. M., Taguchi, S., Tegtmeier, S., Lidster, R. T., Wilson, C., and Ziska, F.: A multi-model intercomparison of halogenated very short-lived substances (TransCom-VSLS): linking oceanic emissions and tropospheric transport for a reconciled estimate of the stratospheric source gas injection of bromine, *Atmos. Chem. Phys. Discuss.*, 2016, 1-49, 10.5194/acp-2015-822, 2016.
- 785 Hughes, C., Franklin, D. J., and Malin, G.: Iodomethane production by two important marine cyanobacteria: *Prochlorococcus marinus* (CCMP 2389) and *Synechococcus* sp. (CCMP 2370), *Marine Chemistry*, 125, 19-25, 10.1016/j.marchem.2011.01.007, 2011.
- 790 James, R., Bonazzola, M., Legras, B., Surbled, K., and Fueglistaler, S.: Water vapor transport and dehydration above convective outflow during Asian monsoon, *Geophysical Research Letters*, 35, 10.1029/2008gl035441, 2008.

- 795 Kim, J., and Son, S.-W.: Tropical Cold-Point Tropopause: Climatology, Seasonal Cycle, and Intraseasonal Variability Derived from COSMIC GPS Radio Occultation Measurements, *Journal of Climate*, 25, 5343-5360, 10.1175/jcli-d-11-00554.1, 2012.
- Krüger, K., and Quack, B.: Introduction to special issue: the TransBrom Sonne expedition in the tropical West Pacific, *Atmospheric Chemistry and Physics*, 13, 9439-9446, 10.5194/acp-13-9439-2013, 2013.
- 800 Latif, M., Syed, F. S., and Hannachi, A.: Rainfall trends in the South Asian summer monsoon and its related large-scale dynamics with focus over Pakistan, *Climate Dynamics*, 1-17, 10.1007/s00382-016-3284-3, 2016.
- 805 Law, K. S., Sturges, W. T., Blake, D. R., Blake, N. J., Burkeholder, J. B., Butler, J. H., Cox, R. A., Haynes, P. H., Ko, M. K. W., Kreher, K., Mari, C., Pfeilsticker, K., Plane, J. M. C., Salawitch, R. J., Schiller, C., Sinnhuber, B. M., von Glasow, R., Warwick, N. J., Wuebbles, D. J., and Yvon-Lewis, S. A.: Halogenated Very Short-Lived Substances, in: *Scientific Assessment of Ozone Depletion: 2006. Global Ozone Research and Monitoring Project - Report N. 50*, World Meteorological Organization, Geneva, Switzerland, 2006.
- 810 Lawrence, M. G., and Lelieveld, J.: Atmospheric pollutant outflow from southern Asia: a review, *Atmospheric Chemistry and Physics*, 10, 9463-9646, 10.5194/acpd-10-9463-2010, 2010.
- 815 Lennartz, S. T., Krysztofiak, G., Marandino, C. A., Sinnhuber, B. M., Tegtmeier, S., Ziska, F., Hossaini, R., Krüger, K., Montzka, S. A., Atlas, E., Oram, D. E., Keber, T., Bönisch, H., and Quack, B.: Modelling marine emissions and atmospheric distributions of halocarbons and dimethyl sulfide: the influence of prescribed water concentration vs. prescribed emissions, *Atmospheric Chemistry and Physics*, 15, 11753-11772, 10.5194/acp-15-11753-2015, 2015.
- Liang, Q., Stolarski, R. S., Kawa, S. R., Nielsen, J. E., Douglass, A. R., Rodriguez, J. M., Blake, D. R., Atlas, E., and Orr, L. E.: Finding the missing stratospheric Bry: a global modeling study of CHBr₃ and CH₂Br₂, *Atmospheric Chemistry and Physics*, 2010.
- 820 Liang, Q., Atlas, E., Blake, D. R., Dorf, M., Pfeilsticker, K., and Schauffler, S.: Convective transport of very short lived bromocarbons to the stratosphere, *Atmospheric Chemistry and Physics*, 14, 5781-5792, 2014.
- Manley, S. L., Goodwin, K., and North, W. J.: Laboratory production of bromoform, methylene bromide, and methyl iodide by macroalgae and distribution in nearshore southern California waters, *Limnology and Oceanography*, 37, 1652-1650, 1992.
- 825 Montzka, S., Butler, J., Hall, B., Mondeel, D., and Elkins, J.: A decline in tropospheric organic bromine, *Geophysical Research Letters*, 30, 2003.
- Moore, R. M., and Zafiriou, O. C.: Photochemical production of methyl iodide in seawater, *Journal of Geophysical Research: Atmospheres*, 99, 16415-16420, 10.1029/94jd00786, 1994.
- 830 Moore, R. M., Geen, C. E., and Tait, V. K.: Determination of Henry's Law constants for a suite of naturally occurring halogenated methanes in seawater, *Chemosphere*, 30, 1183-1191, 10.1016/0045-6535(95)00009-W, 1995a.
- Moore, R. M., Tokarczyk, R., Tait, V. K., Poulin, M., and Geen, C.: Marine phytoplankton as a natural source of volatile organohalogens, in: *Naturally-Produced Organohalogens*, edited by: Grimvall, A., and de Leer, E. W. B., Springer Netherlands, Dordrecht, 283-294, 1995b.
- 835 Moore, R. M., and Groszko, W.: Methyl iodide distribution in the ocean and fluxes to the atmosphere, *Journal of Geophysical Research: Oceans*, 104, 11163-11171, 10.1029/1998jc900073, 1999.

- Munchak, L. A., and Pan, L. L.: Separation of the lapse rate and the cold point tropopauses in the tropics and the resulting impact on cloud top-tropopause relationships, *Journal of Geophysical Research: Atmospheres*, 119, 7963-7978, 10.1002/2013jd021189, 2014.
- 840 Newell, R. E., and Gould-Stewart, S.: A Stratospheric Fountain?, *Journal of the Atmospheric Sciences*, 38, 2789-2796, 10.1175/1520-0469(1981)038<2789:ASF>2.0.CO;2, 1981.
- Nightingale, P., Malin, G., Law, C., Watson, A., Liss, P., Liddicoat, M., Boutin, J., and Upstill-Goddard, R.: In situ evaluation of air-sea gas exchange parameterizations using novel conservative and volatile tracers, *Global Biogeochemical Cycles*, 14, 373-387, 10.1029/1999GB900091, 2000.
- 845 Ordóñez, C., Lamarque, J. F., Tilmes, S., Kinnison, D. E., Atlas, E. L., Blake, D. R., Sousa Santos, G., Brasseur, G., and Saiz-Lopez, A.: Bromine and iodine chemistry in a global chemistry-climate model: description and evaluation of very short-lived oceanic sources, *Atmospheric Chemistry and Physics*, 12, 1423-1447, 10.5194/acp-12-1423-2012, 2012.
- Palmer, C. J., and Reason, C. J.: Relationships of surface bromoform concentrations with mixed layer depth and salinity in the tropical oceans, *Global Biogeochemical Cycles*, 23, 10.1029/2008gb003338, 2009.
- 850 Park, M., Randel, W. J., Gettelman, A., Massie, S. T., and Jiang, J. H.: Transport above the Asian summer monsoon anticyclone inferred from Aura Microwave Limb Sounder tracers, *Journal of Geophysical Research*, 112, 10.1029/2006jd008294, 2007.
- 855 Park, M., Randel, W. J., Emmons, L. K., and Livesey, N. J.: Transport pathways of carbon monoxide in the Asian summer monsoon diagnosed from Model of Ozone and Related Tracers (MOZART), *Journal of Geophysical Research: Atmospheres*, 114, 2009.
- Pearson, K.: Note on Regression and Inheritance in the Case of Two Parents, *Proceedings of the Royal Society of London*, 58, 240-242, 1895.
- 860 Preethi, B., Mujumdar, M., Kripalani, R. H., Prabhu, A., and Krishnan, R.: Recent trends and teleconnections among South and East Asian summer monsoons in a warming environment, *Climate Dynamics*, 1-17, 10.1007/s00382-016-3218-0, 2016.
- Quack, B., and Wallace, D. W. R.: Air-sea flux of bromoform: Controls, rates, and implications, *Global Biogeochemical Cycles*, 17, n/a-n/a, 10.1029/2002gb001890, 2003.
- 865 Quack, B., Atlas, E., Petrick, G., and Wallace, D. W. R.: Bromoform and dibromomethane above the Mauritanian upwelling: Atmospheric distributions and oceanic emissions, *Journal of Geophysical Research*, 112, 10.1029/2006jd007614, 2007.
- Quartly, G. D., Buck, J. J. H., Srokosz, M. A., and Coward, A. C.: Eddies around Madagascar — The retroreflection re-considered, *Journal of Marine Systems*, 63, 115-129, 10.1016/j.jmarsys.2006.06.001, 2006.
- 870 Randel, W. J., Park, M., Emmons, L., Kinnison, D., Bernath, P., Walker, K. A., Boone, C., and Pumphrey, H.: Asian monsoon transport of pollution to the stratosphere, *Science*, 328, 611-613, 10.1126/science.1182274, 2010.
- Roy, R., Pratihary, A., Narvenkar, G., Mochemadkar, S., Gauns, M., and Naqvi, S. W. A.: The relationship between volatile halocarbons and phytoplankton pigments during a *Trichodesmium* bloom in the coastal eastern Arabian Sea, *Estuarine, Coastal and Shelf Science*, 95, 110-118, 10.1016/j.ecss.2011.08.025, 2011.
- 875

- 880 Schauffler, S., Atlas, E., Blake, D., Flocke, F., Lueb, R., Lee-Taylor, J., Stroud, V., and Travnicek, W.:
Distributions of brominated organic compounds in the troposphere and lower stratosphere,
Journal of Geophysical Research-Atmospheres, 104, 21513-21535, 10.1029/1999JD900197, 1999.
- Schott, F. A., Xie, S.-P., and McCreary, J. P.: Indian Ocean circulation and climate variability, *Reviews of
Geophysics*, 47, 10.1029/2007rg000245, 2009.
- 885 Seibert, P., Beyrich, F., Gryning, S., Joffre, S., Rasmussen, A., and Tercier, P.: Review and intercomparison
of operational methods for the determination of the mixing height, *Atmospheric Environment*,
34, 1001-1027, 10.1016/S1352-2310(99)00349-0, 2000.
- Smythe-Wright, D., Boswell, S. M., Lucas, C. H., New, A. L., and Varney, M. S.: Halocarbon and dimethyl
sulphide studies around the Mascarene Plateau, *Philosophical transactions. Series A,
Mathematical, physical, and engineering sciences*, 363, 169-185, 10.1098/rsta.2004.1485, 2005.
- 890 Solomon, S., Garcia, R. R., and Ravishankara, A. R.: On the role of iodine in ozone depletion, *Journal of
Geophysical Research: Atmospheres*, 99, 20491-20499, 10.1029/94jd02028, 1994.
- Stemmler, I., Rothe, M., Hense, I., and Hepach, H.: Numerical modelling of methyl iodide in the eastern
tropical Atlantic, *Biogeosciences*, 10, 4211-4225, 10.5194/bg-10-4211-2013, 2013.
- 895 Stemmler, I., Hense, I., and Quack, B.: Marine sources of bromoform in the global open ocean –
global patterns and emissions, *Biogeosciences Discussions*, 11, 15693-15732, 10.5194/bgd-11-
15693-2014, 2014.
- Stemmler, I., Hense, I., and Quack, B.: Marine sources of bromoform in the global open ocean – global
patterns and emissions, *Biogeosciences*, 12, 1967-1981, 10.5194/bg-12-1967-2015, 2015.
- 900 Stohl, A., Hittenberger, M., and Wotawa, G.: Validation of the Lagrangian particle dispersion model
FLEXPART against large-scale tracer experiment data, *Atmospheric Environment*, 32, 4245-4264,
10.1016/S1352-2310(98)00184-8, 1998.
- Stohl, A., and Thomson, D.: A density correction for Lagrangian particle dispersion models, *Boundary-
Layer Meteorology*, 90, 155-167, 10.1023/A:1001741110696, 1999.
- 905 Stohl, A., and Trickl, T.: A textbook example of long-range transport: Simultaneous observation of ozone
maxima of stratospheric and North American origin in the free troposphere over Europe, *Journal
of Geophysical Research: Atmospheres*, 104, 30445-30462, 10.1029/1999JD900803, 1999.
- Stohl, A., Forster, C., Frank, A., Seibert, P., and Wotawa, G.: Technical note: The Lagrangian particle
dispersion model FLEXPART version 6.2, *Atmospheric Chemistry and Physics*, 5, 2461-2474, 2005.
- Stull, R.: *An Introduction to Boundary Layer Meteorology*, Kluwer Academic Publishers, Dordrecht, 1988.
- 910 Tegtmeier, S., Krüger, K., Quack, B., Atlas, E. L., Pisso, I., Stohl, A., and Yang, X.: Emission and transport of
bromocarbons: from the West Pacific ocean into the stratosphere, *Atmospheric Chemistry and
Physics*, 12, 10633-10648, 10.5194/acp-12-10633-2012, 2012.
- 915 Tegtmeier, S., Krüger, K., Quack, B., Atlas, E., Blake, D. R., Boenisch, H., Engel, A., Hepach, H., Hossaini, R.,
Navarro, M. A., Raimund, S., Sala, S., Shi, Q., and Ziska, F.: The contribution of oceanic methyl
iodide to stratospheric iodine, *Atmospheric Chemistry and Physics*, 13, 11869-11886,
10.5194/acp-13-11869-2013, 2013.
- Vogel, B., Günther, G., Müller, R., Grooß, J. U., and Riese, M.: Impact of different Asian source regions on
the composition of the Asian monsoon anticyclone and on the extratropical lowermost
stratosphere, *Atmospheric Chemistry and Physics*, 15, 13699-13716, 10.5194/acpd-15-13699-
2015, 2015.

- 920 Warwick, N. J., Pyle, J. A., Carver, G. D., Yang, X., Savage, N. H., O'Connor, F. M., and Cox, R. A.: Global modeling of biogenic bromocarbons, *Journal of Geophysical Research: Atmospheres*, 111, 10.1029/2006jd007264, 2006.
- WMO: Definition of the tropopause, *WMO Bull.*, 6, 136, 1957.
- 925 Yamamoto, H., Yokouchi, Y., Otsuki, A., and Itoh, H.: Depth profiles of volatile halogenated hydrocarbons in seawater in the Bay of Bengal, *Chemosphere*, 45, 371-377, 10.1016/S0045-6535(00)00541-5, 2001.
- Yan, R., and Bian, J.: Tracing the boundary layer sources of carbon monoxide in the Asian summer monsoon anticyclone using WRF-Chem, *Adv. Atmos. Sci.*, 32, 943-951, 10.1007/s00376-014-4130-3, 2015.
- 930 Yokouchi, Y., Osada, K., Wada, M., Hasebe, F., Agama, M., Murakami, R., Mukai, H., Nojiri, Y., Inuzuka, Y., Toom-Sauntry, D., and Fraser, P.: Global distribution and seasonal concentration change of methyl iodide in the atmosphere, *Journal of Geophysical Research: Atmospheres*, 113, 10.1029/2008jd009861, 2008.
- 935 Ziska, F., Quack, B., Abrahamsson, K., Archer, S. D., Atlas, E., Bell, T., Butler, J. H., Carpenter, L. J., Jones, C. E., Harris, N. R. P., Hepach, H., Heumann, K. G., Hughes, C., Kuss, J., Krüger, K., Liss, P., Moore, R. M., Orlikowska, A., Raimund, S., Reeves, C. E., Reifenhäuser, W., Robinson, A. D., Schall, C., Tanhua, T., Tegtmeier, S., Turner, S., Wang, L., Wallace, D., Williams, J., Yamamoto, H., Yvon-Lewis, S., and Yokouchi, Y.: Global sea-to-air flux climatology for bromoform, dibromomethane and methyl iodide, *Atmospheric Chemistry and Physics*, 13, 8915-8934, 10.5194/acp-13-8915-2013, 2013.
- 940

945 | **Table 21:** FLEXPART experimental set ups including experiment name, mode, start location and time, runtime, and number of trajectories.

Experiment Name	Mode	Start location	Start time	Runtime	Number of trajectories
<i>OASIS back</i>	Backward; air mass	along ship track	12 UTC, every day during cruise	10 days	50 per cruise day
<i>OASIS</i>	Forward; VLSL	0.0002° x 0.0002° on emission measurements	±30 min from measurement time	10 days (CH ₃ I), 3 months (CHBr ₃), 1.5 years (CH ₂ Br ₂)	10,000 per measurement.
<i>Indian Ocean</i>	Forward; VLSL tracers	1°x1° grid at sea surface; 50°E - 80°E, 20°S - 10°N	Every day from July 1-31, 2000-2015	3 months	29,791 x 16 years

950 | **Table 2:** CHBr₃, CH₂Br₂, and CH₃I water concentrations, air mixing ratios, and calculated emissions for the OASIS Indian Ocean cruise. The table lists the average value of all measurements and 1 standard deviation. The brackets give the range of measurements.

VLSL	Water concentration [pmol L ⁻¹]	Air mixing ratio [ppt]	Emission [pmol m ⁻² hr ⁻¹]
CHBr ₃	8.4 ± 14.2 [1.3 – 33.4]	1.20 ± 0.35 [0.68 – 2.97]	910 ± 1160 [-100 – 9,630]
CH ₂ Br ₂	6.7 ± 12.6 [0.6 – 114.3]	0.91 ± 0.08 [0.77 – 1.20]	930 ± 2000 [-70 – 19,960]
CH ₃ I	3.4 ± 3.1 [0.2 – 16.4]	0.84 ± 0.12 [0.57 – 1.22]	460 ± 430 [5 – 2,090]

Table 3: CHBr₃, CH₂Br₂, and CH₃I mean emissions [pmol m⁻² hr⁻¹] for several cruises and observational and model based climatological studies. Abbreviations: IO = Indian Ocean, OLS = Ordinary Least Square Method

Study	Cruise / Region	CHBr ₃	CH ₂ Br ₂	CH ₃ I
This study	OASIS / West IO	910	930	460
Chuck et al., 2005	ANT XVIII/1 / Tropical Atlantic	125		625
Tegtmeier et al., 2012, 2013	TransBrom / West Pacific Ocean	608	164	320
Hepach et al., 2014	DRIVE / Tropical Atlantic	787	341	254
Hepach et al., 2015	MSM 18/3 / Equatorial Atlantic	644	187	425
Hepach et al., 2016	M91 / Peruvian Upwelling	130	273	954
Fuhlbruegge et al., 2016b	SHIVA / South China Sea	1486	405	433
Quack and Wallace, 2003	Global open ocean	625		
Yokouchi et al., 2005	Global open ocean		119	
Butler et al., 2007	Tropical ocean	379	108	541
Carpenter et al. 2009	Atlantic open ocean	367	158	
Bell et al., 2002	Global ocean			670
Warwick et al., 2006	Tropics, Scenario 5	580		
Liang et al., 2010	Tropics, open ocean, Scenario A	854	81	
Ordoñez et al., 2012	Tropics	956		
Ziska et al., 2013	IO equator, OLS	≈500	≈500	≈250
Ziska et al., 2013	IO subtropics, OLS	≈250	≈250	≈500
Stemmler et al. , 2013	Tropical Atlantic Ocean			≈500
Stemmler et al., 2014	IO equator	≈200		

960 Table 4: Mean Flexpart emission, entrainment at 17 km, transport efficiency, and transit half-life for CHBr_3 , CH_2Br_2 and CH_3I for the mean and different transport regimes of the OASIS cruise.

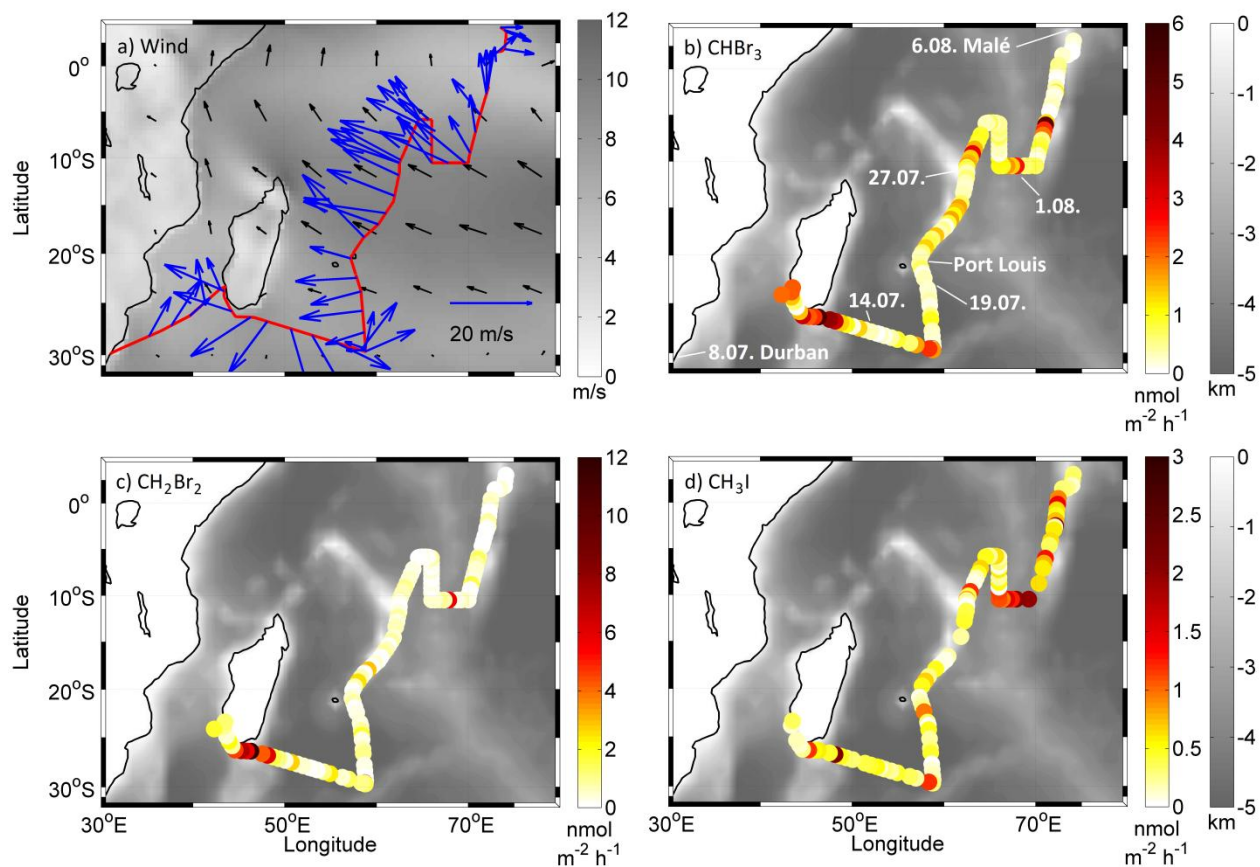
VLS	Transport regime	Flexpart emission [μmol]	Emissions by regime [%]	Transport efficiency [%]	Flexpart entrainment [nmol]	Entrainment by regime [%]	Transit half-life [days]
CHBr_3	Cruise mean	0.43	-	1.283	5.5	-	21
	Westerlies	0.49	32	0.364	1.83	9	32
	Transition	0.36	24	0.586	2.05	11	24
	Monsoon Circulation	0.51	34	2.081	10.70	57	15
	Local Convection	0.15	10	2.869	4.31	23	10
CH_2Br_2	Cruise mean	0.43	-	6.385.5	23.6	-	86
	Westerlies	0.71	48	3.994.00	28.8	35	112
	Transition	0.32	22	4.899	15.0	19	114
	Monsoon Circulation	0.31	21	8.22	26.2	31	63
	Local Convection	0.14	9	8.83	12.7	15	57
CH_3I	Cruise mean	0.22	-	0.253	0.7	-	6
	Westerlies	0.15	18	0.00	0.00	0	9
	Transition	0.11	13	0.00	0.00	0	9
	Monsoon Circulation	0.28	33	0.283	0.74	21	7
	Local Convection	0.31	36	0.951.0	2.77	79	1

965 **Table 5: CHBr₃ entrainment at 17 km for different ocean regions using the same transfer coefficient for the emission calculations and Flexpart model set-up (Sect. 2.2). The table lists the average value and 1 standard deviation. The brackets give the range of single calculations.**

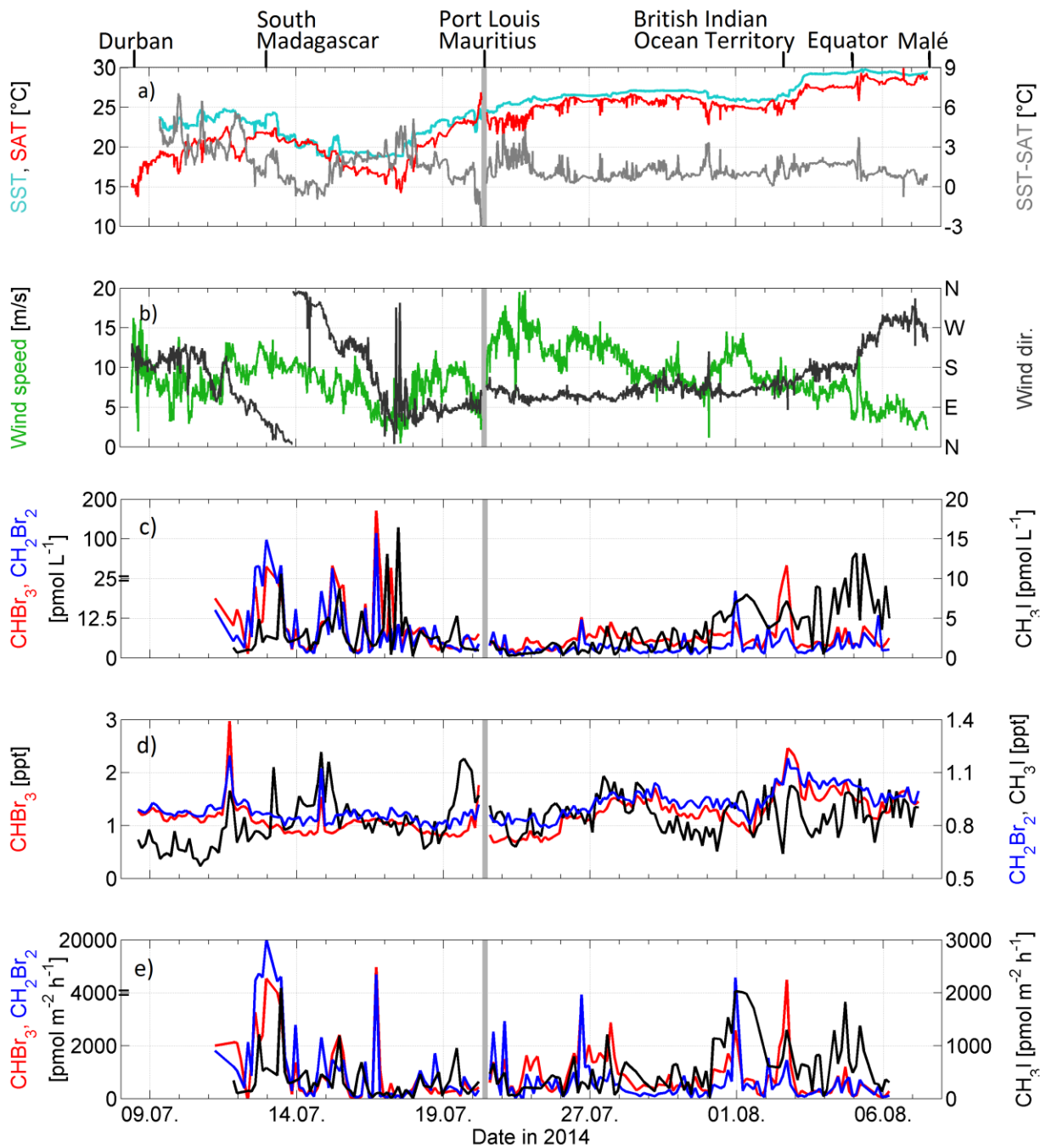
Ocean region	Campaign information	Flexpart emission [nmol]	Flexpart entrainment [nmol]	Transport efficiency [%]
West Indian Ocean	OASIS, July 2014 (this study)	430 ± 520 [4 – 4130]	5.5 ± 7.5 [0.0 – 50.1]	1.4 ± 1.0 [0.1 – 3.9]
Open West Pacific	TransBrom, Oct. 2009 (Krüger and Quack, 2013)	190 ± 300 [0 – 5680]	7.1 ± 10.4 [0.0 – 61.8]	4.4 ± 1.6 [1.9 – 8.8]
Coastal West Pacific	SHIVA, Nov. 2011 (Fuhlbrügge et al., 2016b)	610 ± 720 [1 – 5680]	48.4 ± 52.1 [0.7 – 250.1]	7.9 ± 3.7 [3.2 – 20.2]
Equatorial Atlantic	MSM18/3, June 2011 (Hepach et al., 2015)	320 ± 400 [2 – 1910]	2.7 ± 3.2 [0.0 – 14.2]	0.9 ± 0.2 [0.5 – 1.4]

970 **Table 6: Entrainment of CHBr₃, CH₂Br₂ and CH₃I tracer at 17 km altitude through different transport regimes from the West Indian Ocean release box. Correlations with significance of more than 95% are marked in bold. (Note, transit half-lives differ from Table 4 because of the different model setups.)**

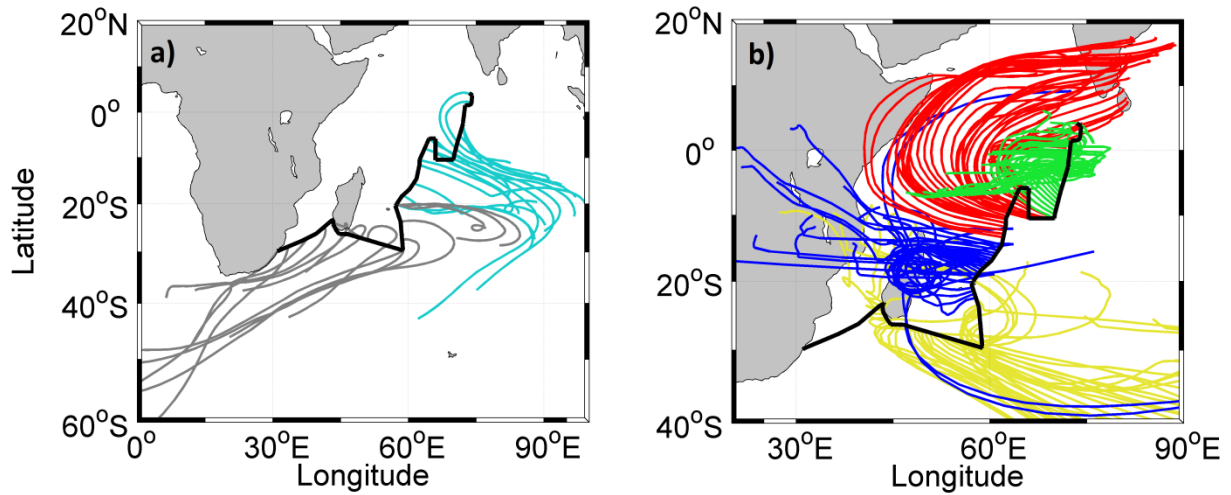
Tracer	Transport regime	Mean transport efficiency [%]	Transit half-life [days]	Interannual correlation with <i>Total</i> entrainment	Interannual correlation with <i>Local Convection</i> entrainment
CHBr ₃	<i>Total</i>	1.86	8.5	1.00	0. 39 <u>45</u>
	<i>Local Convection</i>	0. 20 <u>24</u>	2.5 <u>1.8</u>	0. 39 <u>45</u>	1.00
	<i>Monsoon Circulation</i>	0.50	6.0	0.54	-0. 23 <u>20</u>
CH ₂ Br ₂	<i>Total</i>	5.88	27.2	1.00	0. 17 <u>24</u>
	<i>Local Convection</i>	0. 28 <u>32</u>	3.8 <u>2.4</u>	0. 17 <u>24</u>	1.00
	<i>Monsoon Circulation</i>	1.11	13.3	0.56	-0. 11 <u>06</u>
CH ₃ I	<i>Total</i>	0.42	1.9	1.00	0.8791
	<i>Local Convection</i>	0. 14 <u>17</u>	1. 6 <u>2</u>	0.8791	1.00
	<i>Monsoon Circulation</i>	0.09	1.0	-0.06	-0. 29 <u>31</u>



975 **Figure 1: a) July 2014 average wind speed (grey shading) and direction (black) from ERA-Interim and 10 min mean wind speed (blue arrows) from ship sensors; b) CHBr_3 , c) CH_2Br_2 , and d) CH_3I emissions derived from OASIS cruise July-August 2014 and bathymetry.**



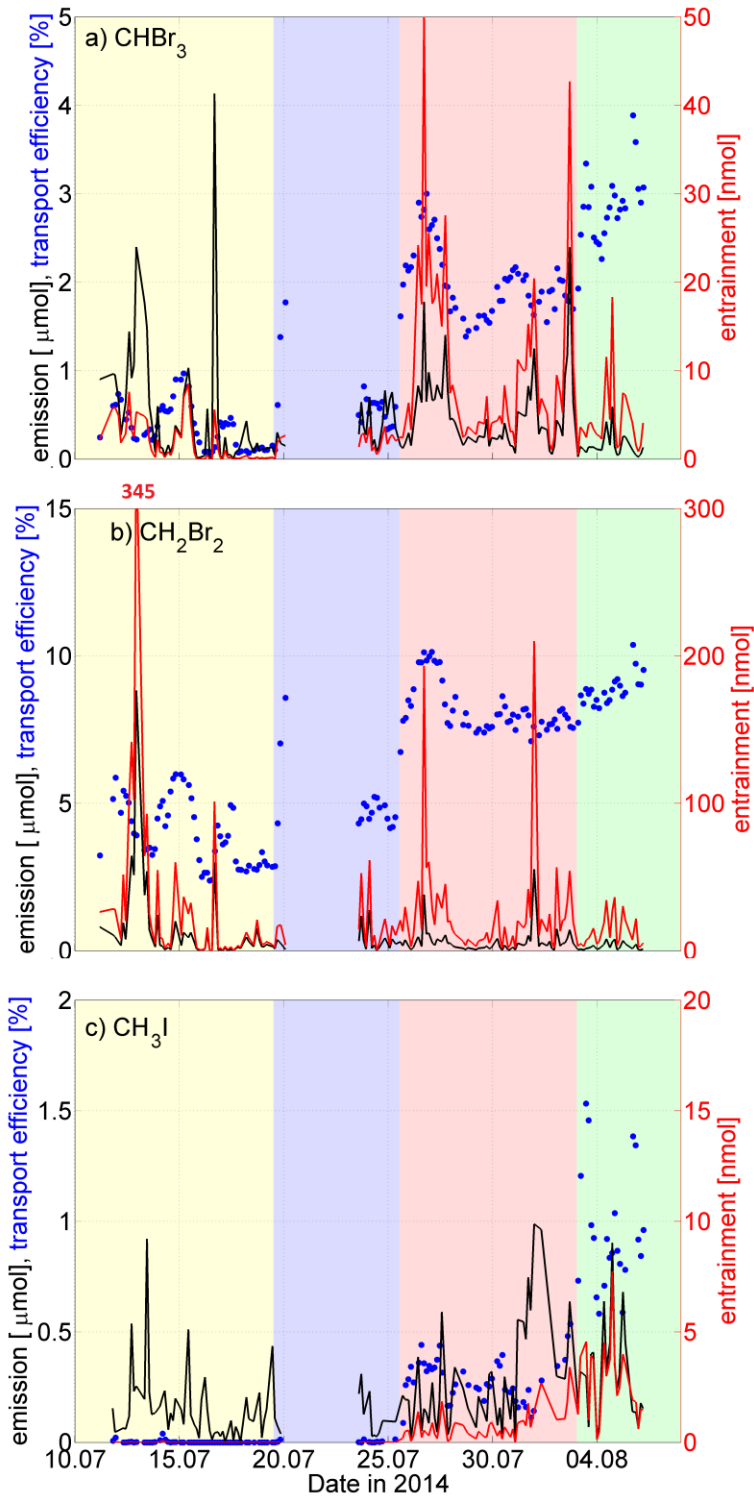
980 **Figure 2:** a) Surface air temperature (SAT), sea surface temperature (SST), b) wind speed and direction measured by ship sensors during the OASIS cruise in the Indian Ocean. c) Water concentration, d) atmospheric mixing ratio and e) emission of CHBr_3 , CH_2Br_2 , and CH_3I . The grey line denotes the harbor stop at Port Louis, Mauritius, July 20-23, 2014. Also note the nonlinear left y-axes in c) and e).



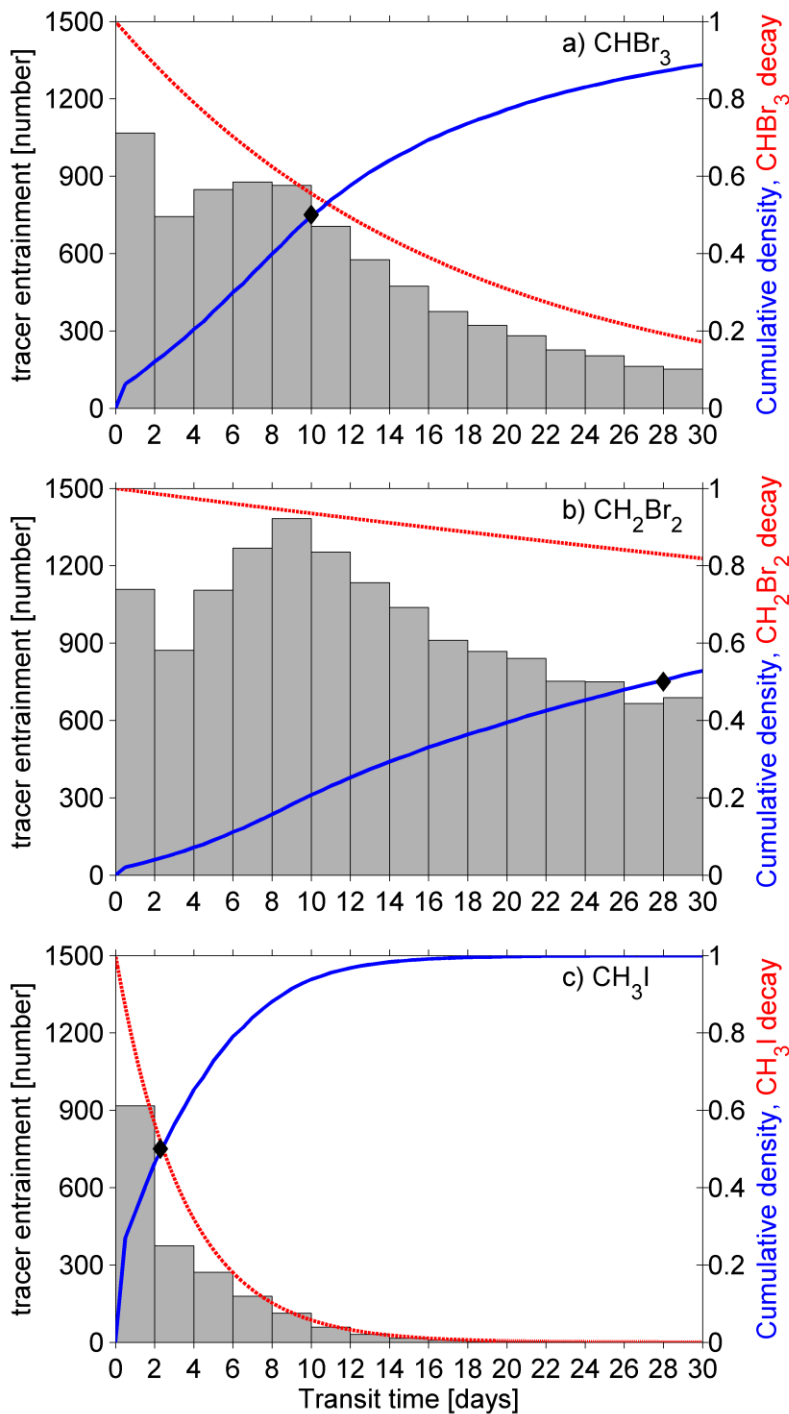
985

Figure 3: a) Flexpart five day backward trajectories for *OASIS backward* setup, averaged for $n=50$ trajectories, starting from ship positions daily at 12 UTC between July 8 and August 7, 2014. The Southern Ocean (grey) and the Open Indian Ocean (turquoise) are source regions for air measured during the cruise. b) Flexpart ten day forward trajectories for *OASIS* setup, averaged for $n=1000$ trajectories, starting at the ship positions of simultaneous VLSL measurements. Trajectories are colored according to their transport regimes: **Westerlies**, **Transition**, **Monsoon Circulation**, and **Local Convection**.

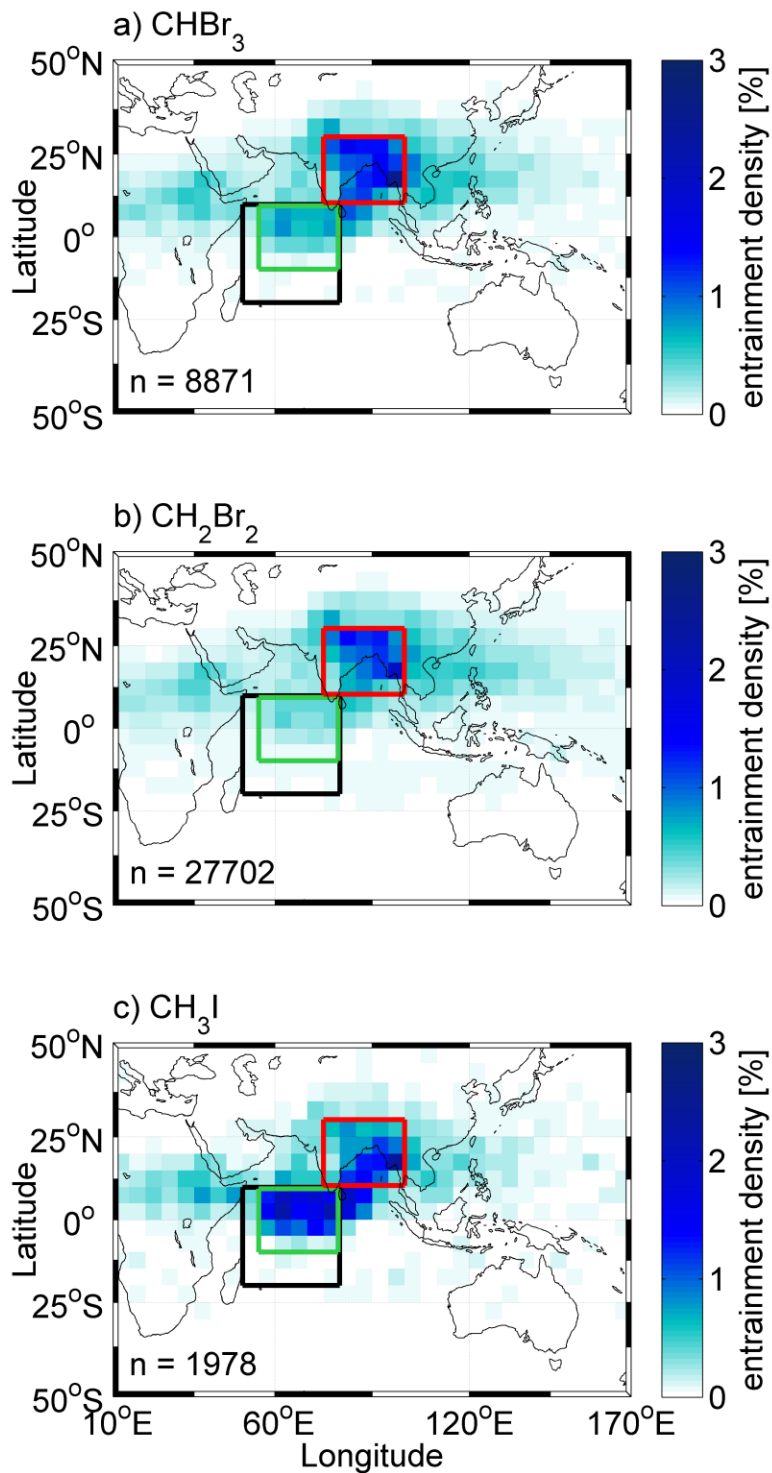
990



995 **Figure 4: CHBr_3 , CH_2Br_2 , and CH_3I emission, entrainment at 17 km and transport efficiency for measurements from the OASIS cruise. The background shading highlights the transport regimes: **Westerlies**, **Transition**, **Monsoon Circulation**, and **Local Convection**.**

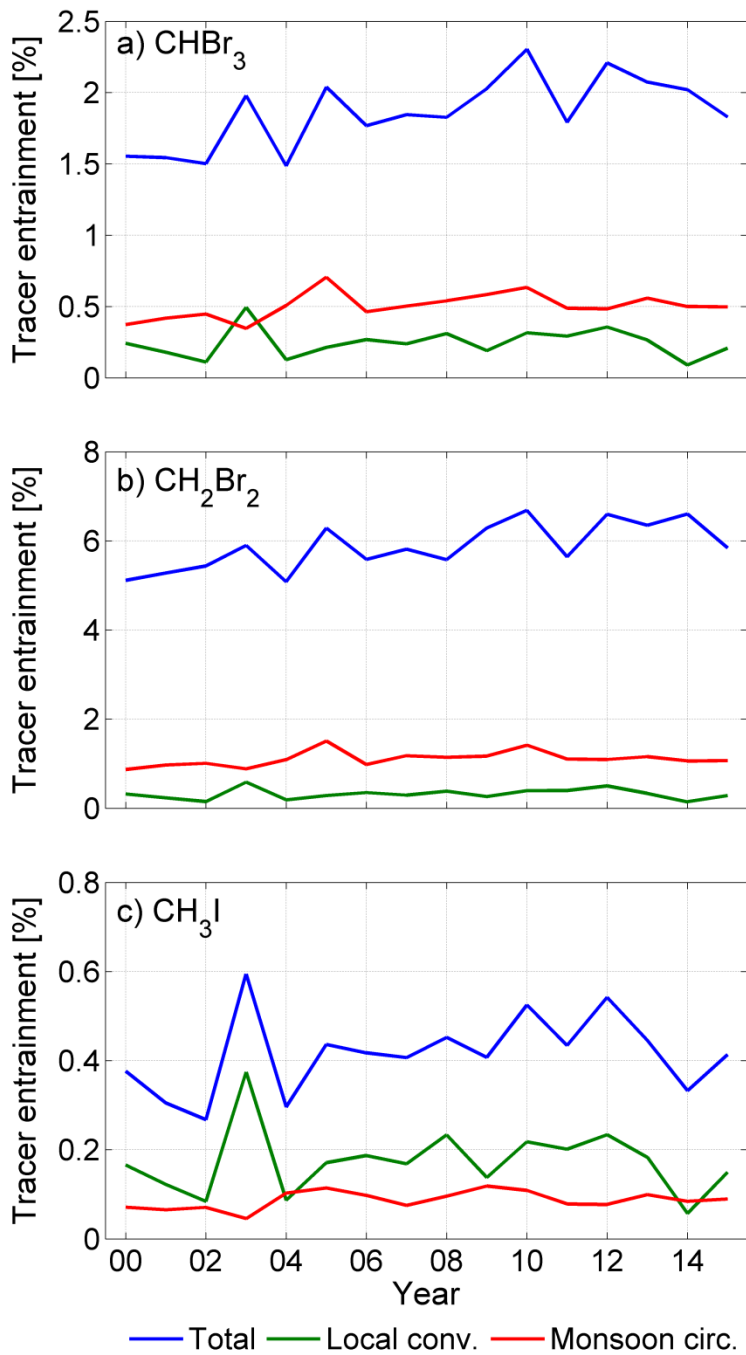


1000 **Figure 5: VLSL transit time distribution for entrainment at 17 km of a) CHBr₃, b) CH₂Br₂, and c) CH₃I tracers released in July 2000-2015. Entrained tracer per time interval of 2 days is given as number (grey bars). The blue line gives the cumulative distribution and denotes the transit half-life. The red line shows the decay of the tracers during the transport simulation. The black diamond denotes the transit half-life.**



1005

Figure 6: Density at 17 km of a) CHBr_3 , b) CH_2Br_2 , and c) CH_3I tracer on a $5^\circ \times 5^\circ$ grid that is released from the West Indian Ocean surface (black box) in July, 2000-2015. Colored boxes show the entrainment regions of the **Local Convection** and **Monsoon Circulation** regimes.



1010

Figure 7: a) CHBr₃, b) CH₂Br₂, and c) CH₃I tracer entrainment at 17 km from trajectories released from the West Indian Ocean surface box in July 2000 - 2015. The entrainment is evaluated for three regions: Total, Local Convection, and Monsoon Circulation (see Fig. 6).

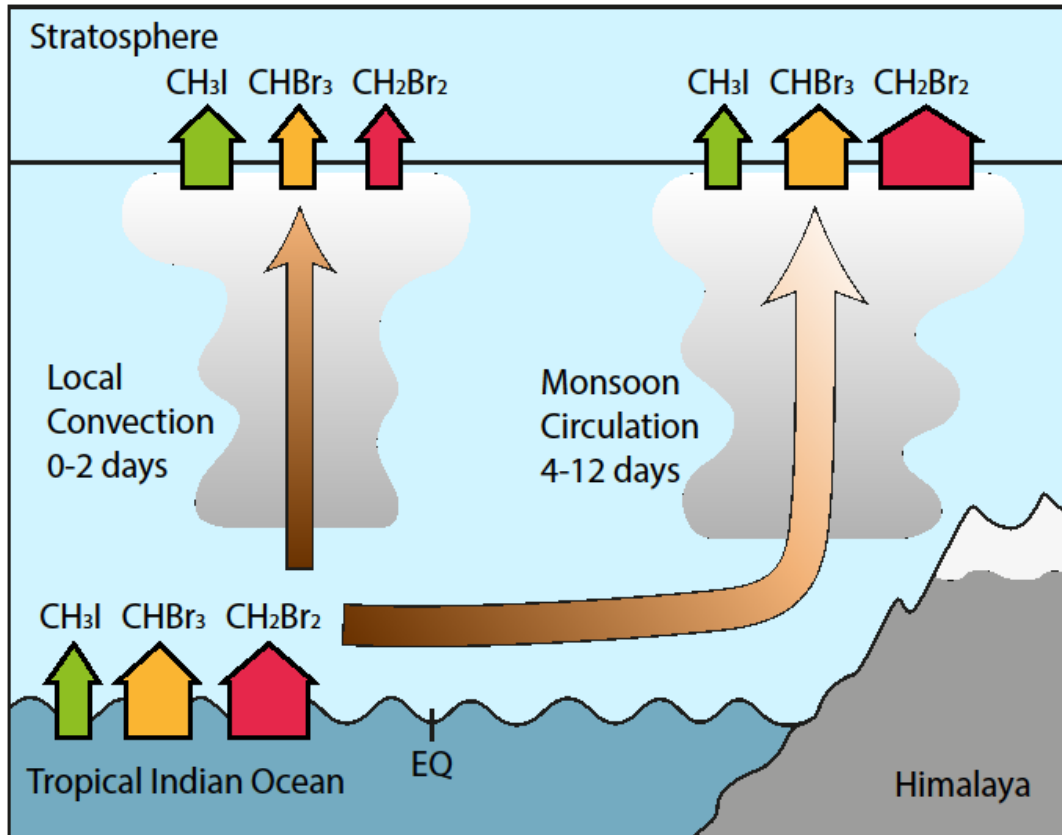


Figure 8: Schematic illustration of emission, transport pathways and timescales, and entrainment of CH_3I , CHBr_3 , and CH_2Br_2 tracer from the tropical West Indian Ocean to the stratosphere during the Asian summer monsoon.